OAK RIDGE
NATIONAL LABORATORY
MANAGED BY UT-BATTELLE
FOR THE DEPARTMENT OF ENERGY

ORNL/TM-2001/9

Advanced Ultrasonic Inspection Techniques for General Purpose Heat Source Fueled Clad Closure Welds

M. William Moyer

UT-BATTELLE
ORNL-27 (4-00)

TM-2001/9

Advanced Ultrasonic Inspection Techniques for General Purpose Heat Source Fueled Clad Closure Welds

M. William Moyer
Characterization and Analysis Technologies Department
Technology Development Division
Y-12 National Security Complex

February 14, 2001

Prepared by the
Oak Ridge National Laboratory
Oak Ridge, Tennessee 37831-6079
operated by UT-Battelle, LLC
for the
U. S. DEPARTMENT OF ENERGY
under contract DE-AC05-00OR22725

CONTENTS

LIST OF FIGURES

LIST OF TABLES

ABSTRACT

A radioisotope thermoelectric generator is used to provide a power source for long-term deep space missions. This General Purpose Heat Source (GPHS) is fabricated using iridium clad vent sets to contain the plutonium oxide fuel pellets. Integrity of the closure weld is essential to ensure containment of the plutonium. The Oak Ridge Y-12 Plant took the lead role in developing the ultrasonic inspection for the closure weld and transferring the inspection to Los Alamos National Laboratory for use in fueled clad inspection for the Cassini mission.

Initially only amplitude and time-of-flight data were recorded. However, a number of benign geometric conditions produced signals that were larger than the acceptance threshold. To identify these conditions, a B-scan inspection was developed that acquired full ultrasonic waveforms. Using a test protocol the B-scan inspection was able to identify benign conditions such as weld shield fusion and internal mismatch. Tangential radiography was used to confirm the ultrasonic results. All but two of 29 fueled clads for which ultrasonic B-scan data was evaluated appeared to have signals that could be attributed to benign geometric conditions. This report describes the ultrasonic inspection developed at Y-12 for the Cassini mission.

INTRODUCTION

Spacecraft destined for deep space exploration cannot effectively use solar power as an energy source due to their distance from the sun. In addition, some satellites and planetary space probes operating close to the sun have electrical power design requirements that cannot withstand cyclical solar exposures or rely on rechargeable batteries. Furthermore, as the electrical power requirements for spacecraft increase, the capability of solar power to supply the electricity becomes limited by the size of the solar panels. Therefore, a reliable, long-term supply of energy is required.

The U.S. civilian space program has employed radioisotope thermoelectric generators (RTGs), which contain the isotope plutonium-238 (^{238}Pu). The natural decay of ^{238}Pu is used to power the systems and components through conversion of decay heat to electricity via thermocouples.[1] The RTG and the power conversion components do not contain any moving parts and do not require maintenance or manual operation. To the extent possible, current RTG designs maximize immobilization of the fuel during all mission phases, including ground transportation and handling, launch operations, and any possible reentry accidents. The design reflects the intent of safety criteria that require fuel containment with a high probability of minimizing leakage during all mission phases.

Between June 1961 and October 1997, the United States launched a total of 25 nuclear power sources, 8 of which involved manned spacecraft. The latest efforts include the 1989 and 1990 launches of Galileo and Ulysses and the October 1997 launch of the Cassini interplanetary probe to Saturn. The RTGs for Galileo and Ulysses were made in the early 1980's while the RTGs for Cassini were made in the mid 1990's. The Cassini mission required approximately 900 W of electrical power to supply its instruments and components. This power is provided by three RTGs. Each RTG contains approximately 22 kg of ^{238}Pu and consists of 72 General Purpose Heat Source (GPHS) iridium capsules, each containing a pellet of plutonium oxide ($^{238}PuO_2$). The iridium capsules are sealed with a circumferential girth weld to hermetically contain the $^{238}PuO_2$. Each GPHS capsule is designed to produce approximately 60 watts thermal at a temperature of 1287°C. Each RTG assembly is designed to produce a maximum of 300 watts of electricity.

The iridium capsule that contains the $^{238}PuO_2$ pellets in the RTG is an important component because it provides for pellet containment during impact in an accident. The integrity of the girth weld is of concern. The design of the RTGs for Cassini is the same as that used for the RTGs of Galileo and Ulysses, and the safety analyses are based on the Galileo/Ulysses RTG configuration. Thus, it is important to use, wherever possible, the same testing configurations as those used for Galileo/Ulysses.

Past experience indicated the potential for some iridium alloy batches to crack in the weld. Although the cracking problem apparently has been solved, an inspection of the girth weld is still required. An ultrasonic inspection was used for the Galileo/Ulysses capsules. Unfortunately, it was difficult to duplicate the Galileo/Ulysses inspection configuration. Oak Ridge National Laboratory (ORNL) and the Y-12 National Security Complex (Y-12) were involved in the procurement and fabrication of the iridium capsule material, verification of the weldability of the iridium, and development of the ultrasonic test to certify the closure weld in the capsule. This report reviews the work at Y-12 to determine and characterize the ultrasonic inspection techniques used for the Galileo/Ulysses capsules and to develop and implement a suitable ultrasonic inspection of the GPHS capsule girth weld for the Cassini GPHS capsules.[2] In addition, this report describes the effort to develop a B-scan inspection to discriminate between benign and detrimental conditions in the weld.

DEVELOPMENT OF THE ULTRASONIC INSPECTION AT Y-12 FOR CASSINI FUELED CLADS

History

Figure 1 is a drawing of the iridium GPHS fueled clad, which consists of two cups that are welded together in the final assembly. One of the cups has a vent shield assembly, which allows the escape of helium that is a product of the decay of the $^{238}PuO_2$ fuel. A thin foil of iridium with three weld tabs was held in place by tack welds to form a shield behind the weld to prevent the weld from spiking into the $^{238}PuO_2$ pellet. The Cassini design is similar to the Galileo/Ulysses design except that the weld shield is formed to fit around the $^{238}PuO_2$ pellet to eliminate the need for tack welds.

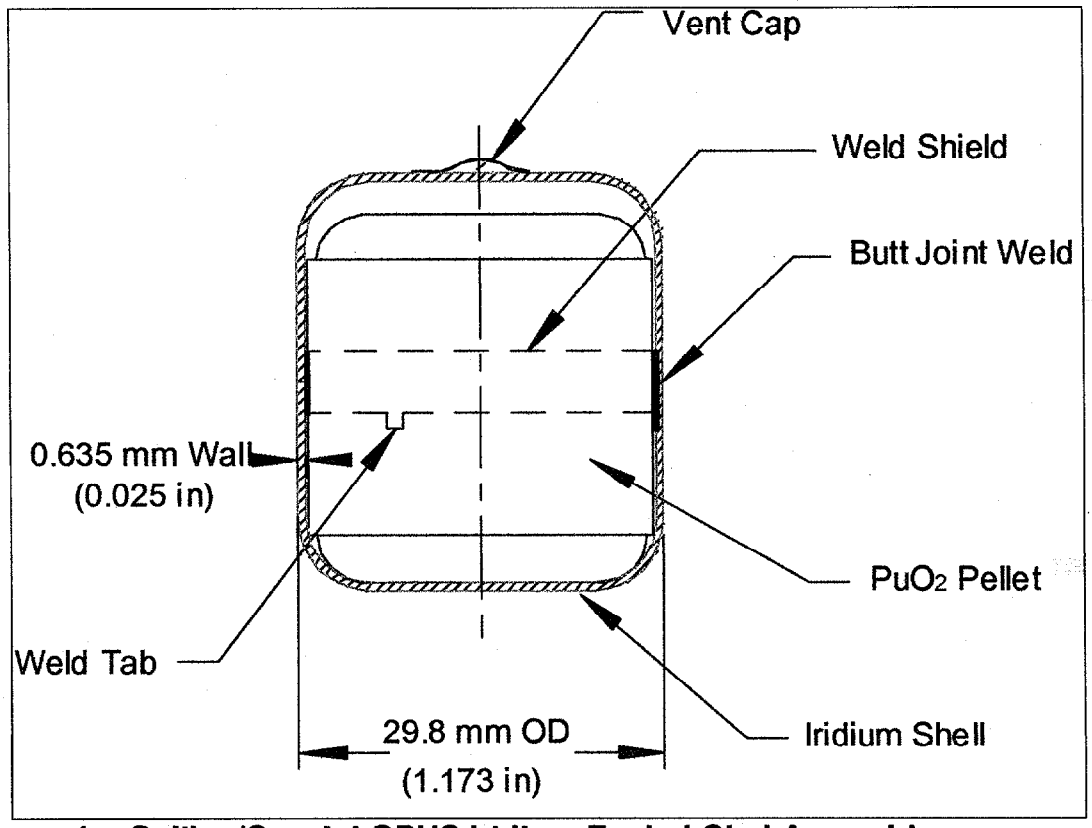

Figure 1 – Galileo/Cassini GPHS Iridium Fueled Clad Assembly

In this report, capsules that contain a PuO_2 pellet are referred to as fueled clads. Empty c`apsules are referred to as clad vent sets (CVS). The GPHS fueled clads for the Galileo/Ulysses programs were made at the Savannah River Plant, which is now referred to as the Savannah River Site (SRS). In the early phases of production, cracks were observed on the underbead in the arc quench area of production GPHS welds. When a new batch of iridium alloy was introduced, the

rejection rate soared to 50%. The cracks were noted only in the weld-overlap area. Upon examination of the cracks it was concluded that they were a result of thermal and solidification stresses that led to weld quench cracking. The cracks were not visible on the external surface of the weld and, if left undetected, could compromise the containment of the $^{238}PuO_2$ in the unlikely event of an aborted launch or re-entry into the earth's atmosphere. Changing the iridium alloy batch and switching to a four-pole oscillator on the welder reduced the rejection rate to an acceptable level.

An ultrasonic test was developed to reject grossly cracked samples and to verify the absence of cracks in the weld after the welding process was brought under control.[3] This ultrasonic inspection was used to indicate the weld quality, rating each weld in terms of a reference slot in a standard. The threshold was set at a "number 8," which is apparently 80% of the response from a 0.152 mm (0.006 in.) deep by 0.25 mm (0.010 in.) wide slot in the standard. Each fueled clad was given a rating related to the number 8 reference. The initial intent of the ultrasonic test was to weed out large cracks in the weld overlap area. Reviews of the Galileo data indicate that reporting the largest indication found, no matter where on the weld perimeter it occurred, became the practice.

An inspection system was designed to hold the fueled clad with the axis of rotation in the horizontal position. A lathe was used to rotate the fueled clad. An arm that held the transducer at a fixed angle could be moved into place to allow a single circumferential scan of the fueled clad. The axial position of the transducer was adjusted manually. A 5.0-MHz transducer with a 19.1 mm (0.75 in.) focal length in water was used for the inspection. The transducer was mounted with the axis tilted 31 degrees from the normal to the fueled clad surface. This angle is just past the shear critical angle for iridium and would produce Rayleigh or Lamb waves in the fueled clad.

The ultrasonic instrumentation described in the SRS procedures was obsolete, and the tooling and fixturing to hold and scan the parts were no longer available. The original part fixturing was extremely difficult to set up and adjust and only produced a single line scan from the weld. The instrument output was recorded on a strip chart recorder. For the Galileo/Ulysses inspection, only a single reference slot was used to calibrate the instrumentation. To better quantify a defect size, several reference slots of different sizes that span the range of expected defect sizes should be used for calibration to verify the linearity of the instrumentation and provide confidence in the testing procedure.

Because the Y-12 National Security Complex had the equipment and experience to inspect thin metal welds,[4] it was asked to review the procedures used to inspect Galileo/Ulysses GPHS fueled clads. Y-12 was then asked to acquire and install the fixturing, instrumentation, data acquisition, and analysis equipment to set up a viable inspection for the Cassini GPHS fueled clads. Y-12 was also involved in the fabrication of the iridium alloy clad vent sets. The DOP-26

iridium-base alloy containing nominally 0.3 weight % tungsten, 60 wppm thorium, and 50 wppm aluminum was developed at Oak Ridge National Laboratory (ORNL).

C-Scan Ultrasonic Inspection Development for Cassini

Since the SRS equipment and standards were unavailable for the Cassini inspection and the ultrasonic inspection technique developed for Galileo/Ulysses suffered from several problems, Y-12 investigated the inspection geometry to optimize the inspection. A mock-up CVS was welded and made available along with a reference CVS that contained three electro-discharge machined slots. The reference CVS was not used for the Galileo/Ulysses calibration, and its history is unknown.

Table 1 summarizes the acoustic properties of iridium. Table 2 summarizes the wavelength of sound in iridium for several frequencies. A reference CVS with several electro-discharge machined slots on the ID surface was fabricated and used to develop the inspection.

Table 1 – Acoustic Properties of Iridium

Velocities				
Longitudinal Velocity	5.305	mm/μs	0.2089	in/μs
Shear Velocity	3.119	mm/μs	0.1228	in/μs
Rayleigh Velocity	2.862	mm/μs	0.1127	in/μs
Extensional Velocity	4.904	mm/μs	0.1931	in/μs
Material Properties				
Young's Modulus	541.36	GPa	78.517	Mpsi
Shear Modulus	219.02	GPa	31.766	Mpsi
Bulk Modulus	341.59	GPa	49.543	Mpsi
Poisson's Ratio	0.236			
Density	22.514	gm/cm^3		
Longitudinal Acoustic Impedance	11.944	gm/cm^2-μs		
Shear Acoustic Impedance	7.022	gm/cm^2-μs		
Longitudinal Critical Angle	16.2	degrees		
Shear Critical Angle	28.33	degrees		
Rayleigh Wave Critical Angle	31.14	degrees		

Since Y-12 has had success with a 45-degree shear inspection for detecting lack-of-penetration, a 45-degree shear wave inspection was investigated. This test is capable of giving a linear response to lack-of-penetration that is less than 0.707 times the acoustic wavelength. Using both 5 and 10 MHz transducers, the reference CVS was inspected with an incident angle of 19.6 degrees. From Table 2, this produces a 45 degree shear wave within the wall of the CVS that is sensitive to lack-of-penetration up to 0.44 mm (0.017 in.) for 5 MHz and 0.22 mm (0.0086 in.) for 10 MHz. Although both frequencies are adequate to detect the

required 0.156 mm (0.006 in.) standard slot, the 10 MHz transducer has better resolution. However, the time separation between the signal from the reference electro-discharge machined slots and the front surface indications from the weld surface roughness was insufficient to resolve the slots. Thus, setting the gate to detect weld defects in the presence of the outside surface weld bead was very difficult. Consequently, the shear wave inspection was not recommended.

Table 2 – Iridium Wavelength Calculations

MHz	Longitudinal Wavelength		Shear Wavelength		Rayleigh Wavelength	
	mm	inch	mm	inch	mm	inch
1.00	5.305	0.2089	3.119	0.1228	2.862	0.1127
2.25	2.358	0.0928	1.386	0.0546	1.272	0.0501
3.50	1.516	0.0597	0.891	0.0351	0.818	0.0322
4.00	1.326	0.0522	0.780	0.0307	0.716	0.0282
5.00	1.061	0.0418	0.624	0.0246	0.572	0.0225
7.50	0.707	0.0278	0.416	0.0164	0.382	0.0150
10.00	0.531	0.0209	0.312	0.0123	0.286	0.0113

Next, in an attempt to reproduce the inspection originally used at SRS for Galileo/Ulysses fueled clads an inspection at 31.1 degrees was tried. This inspection angle will produce Rayleigh or Lamb waves depending upon the inspection frequency and part thickness. Above 5 MHz, where the wavelength is less than the wall thickness of the iridium capsule, Rayleigh waves are generated which penetrate approximately one wavelength into the capsule wall. Thus, above 5 MHz, defects on the inside wall may not be detected. For thinner samples, or at lower frequencies, the ultrasonic energy interacts with both bounding surfaces of the capsule wall simultaneously. Under these conditions, nondispersive bulk-wave propagation is replaced by a fundamentally different form of elastic guided wave propagation, i.e., by Lamb wave propagation.[5]

In the 3.5- to 5.0-MHz frequency range, a Lamb wave mode is generated. Signals from the reference electro-discharge machined slots gave a characteristic signal with a center frequency of approximately 4 MHz, which was delayed from the weld surface noise. This frequency corresponds to a wavelength that matches the capsule wall thickness. Dropping the inspection frequency from 5 MHz to 3.5 MHz produced better sensitivity and a more linear response to the electro-discharge machined slot size in the reference CVS. From Table 2, the wavelength of Rayleigh waves in iridium from the 3.5 MHz transducer more closely matches the part wall thickness than the wavelength of the 5.0-MHz transducer. Also, there is more 4 MHz energy obtained from the 3.5 MHz transducer than from the 5.0 MHz transducer. Standard transducers in this frequency range are only available with center frequencies of 3.5 and 5.0 MHz. Because the maximum wall thickness can be up to 0.71 mm (0.028 in.), the lower frequency for inspection seemed appropriate.

The three slots in the reference CVS were adjacent to the top side of the weld. An inspection was made from both above and below the weld in the reference CVS using the 3.5-MHz Lamb wave inspection. All three electro-discharge machined slots adjacent to the weld could be seen. The sensitivity to the smaller electro-discharge machined slots was reduced in the scan from below the weld. This result is caused by the sound being attenuated by the weld before being reflected from the slot. Thus, the author recommended that both the standard and the welds be inspected from both sides of the weld so that the larger signal from each defect or reference slot would then be used to judge the weld quality. Inspection of the mock-up CVS from the top side (Vent Up) indicated three equally spaced signals from the three spot welds used to hold the thin iridium weld shield.

A 20-MHz, normal longitudinal inspection was used to look at weld contour and for internal defects in the mock-up CVS. The inspection was set up to record both the amplitude and the time of the back surface signal. Because the weld surface is not machined, the normal inspection was more sensitive to the outside surface contour of the weld bead than to the weld-root contour. In addition, iridium used for GPHS fueled clads is a large-grained material and thus quite attenuative at the higher frequencies (20 and 30 MHz) required to separate the back surface signal from the front surface signal. The amplitude scan showed significant variations in the material attenuation around the part in the base material away from the weld. It also showed significant attenuation near the weld edges, apparently as a result of weld-bead contour. The high attenuation of the material caused the instrumentation to lose the back surface signal in a large area of the weld so that it was not possible to map adequately the CVS thickness and weld-root contour in the weld area. Because the normal longitudinal inspection would be a difficult inspection to implement in the production environment and the information provided by the inspection would be difficult to interpret, the normal inspection was not recommended. However, for future programs, the normal inspection might be used to detect the capsule internal mismatch condition described later in this report.

Once an inspection technique was chosen, a considerable effort was required to optimize the inspection and translate it into a production test. This effort included design and fabrication of standards, procurement of an inspection system, development of a testing procedure, programming of the data analysis, and correlation (if possible) of current inspection results with results obtained for Galileo/Ulysses fueled clads. This effort was complicated by the requirement for inspection capabilities at three different sites: SRS, Los Alamos National Laboratory (LANL), and Y-12. To meet these requirements, four sets of standards were designed and made. To simplify the data analysis and to automate the inspection, four identical computer-controlled scanning, data acquisition and analysis systems were specified and procured.

The ultrasonic standards were fabricated to include a slot that matched the geometry of slot in the original standard (0.25 mm, 0.010 in. wide) as well as narrow 0.10 mm (0.004 in.) wide slots that were of optimum geometry for the test. Using the slots, the inspection setup was optimized. The optimization process included transducer frequency, incident angle, and water path. Temperature effects were also considered. At 5.0 MHz, significant interference was noted particularly from the wider test slots. For instance, in some cases the signal from a 0.229 mm (0.009 in.) slot was smaller than the signal from a 0.152 mm (0.006 in.) slot. The best results were obtained using 3.5 MHz at an inspection angle of 32.15 degrees.

The new inspection system was set up to obtain four scans as shown in Figure 2. Scans were made from both sides of the weld to minimize attenuation of indications by the weld. The Left and Right scans were proposed to detect indications or cracks parallel to the fueled clad axis. These scans were subsequently dropped.

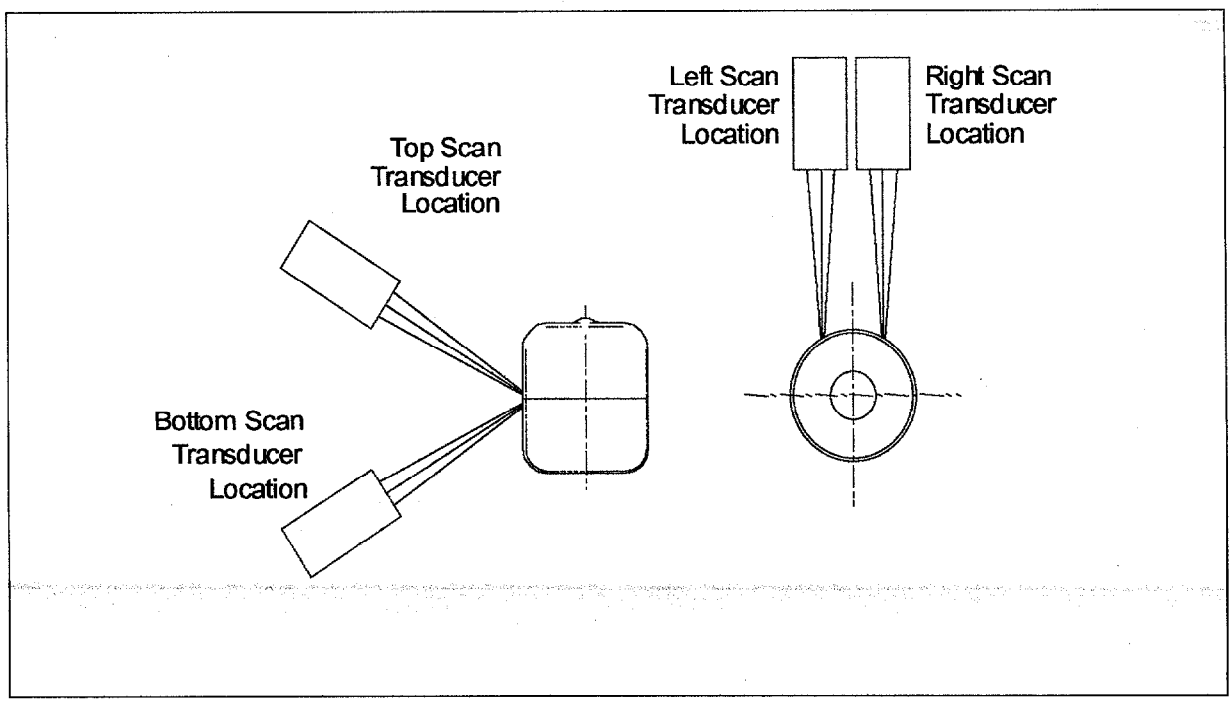

Figure 2 – Initial Scan Setup

Tests were also performed to duplicate the setup used at SRS. These tests were used to estimate depth of a 0.1 mm (0.004 in.) wide slot that produced the same amplitude as that obtained from the 0.25 mm (0.010 in.) wide "number 8 flaw" used as a threshold for the original Galileo/Ulysses inspection. It was determined that a threshold of 0.132 mm (0.0052 in.) corresponded to the "number 8 flaw."

Time-of-Flight Inspection

After all efforts to optimize the inspection configuration were implemented at LANL, a concern still existed that the ultrasonic inspection technique may produce false calls on nonexistent or subsize flaws, or benign conditions such as suckback, weld protrusion, internal wall mismatch and weld shield fusion. This would cause unnecessary rejection of fueled clad welds. All efforts to duplicate the Galileo/Ulysses configuration showed that similar problems might have occurred for the Galileo/Ulysses inspection. The author has shown that interference effects occur at 5.0 MHz and that at both 3.5 and 5.0 MHz, innocuous conditions and weld surface perturbations from the edge of the weld can produce signals that exceeded the reject threshold. Arnost Placr, a WSRC engineer, experimented with sending sound into the radius (knuckle) at the top of the capsule. This experiment produced an inspection mode that simplified the test and seemed to reduce the interference of signals from benign conditions of weld geometry. The test depends upon the generation of Lamb waves at the capsule knuckle. The Lamb wave then travels down the wall of the capsule to the weld. Any reflections from defects in the weld are separated in time from the entry surface signal (at the knuckle) by the travel time along the length of the capsule wall from the knuckle to the weld, which is determined by the Lamb wave velocity. This process enables the signals from the weld to be separated from the front surface signal.

Top Scan Lamb Wave inspection Configuration

Initially, an inspection was set up with the focused transducer angled at 36 degrees above horizontal scanning past the knuckle along the vertical (Z) axis as shown on the left side of Figure 3. As the beam swept across the knuckle region of the capsule, Lamb waves were generated that matched the geometry and incident wave conditions. Because the beam of the focused transducer has a half angle of approximately 8 degrees, the incident energy is incident at a range of angles of 28 to 44 degrees. The test setup was verified using the reference slots in the standards.

The test setup was optimized by adjusting the angle and the water path. The 36-degree angle produced the best results. The problem with the setup was that as the transducer was translated along the Z-axis, the point at which the beam was incident upon the knuckle of the capsule also moved. This caused the distance from the incident point to the reference slots in the standard to change so that the time to the signal changed.

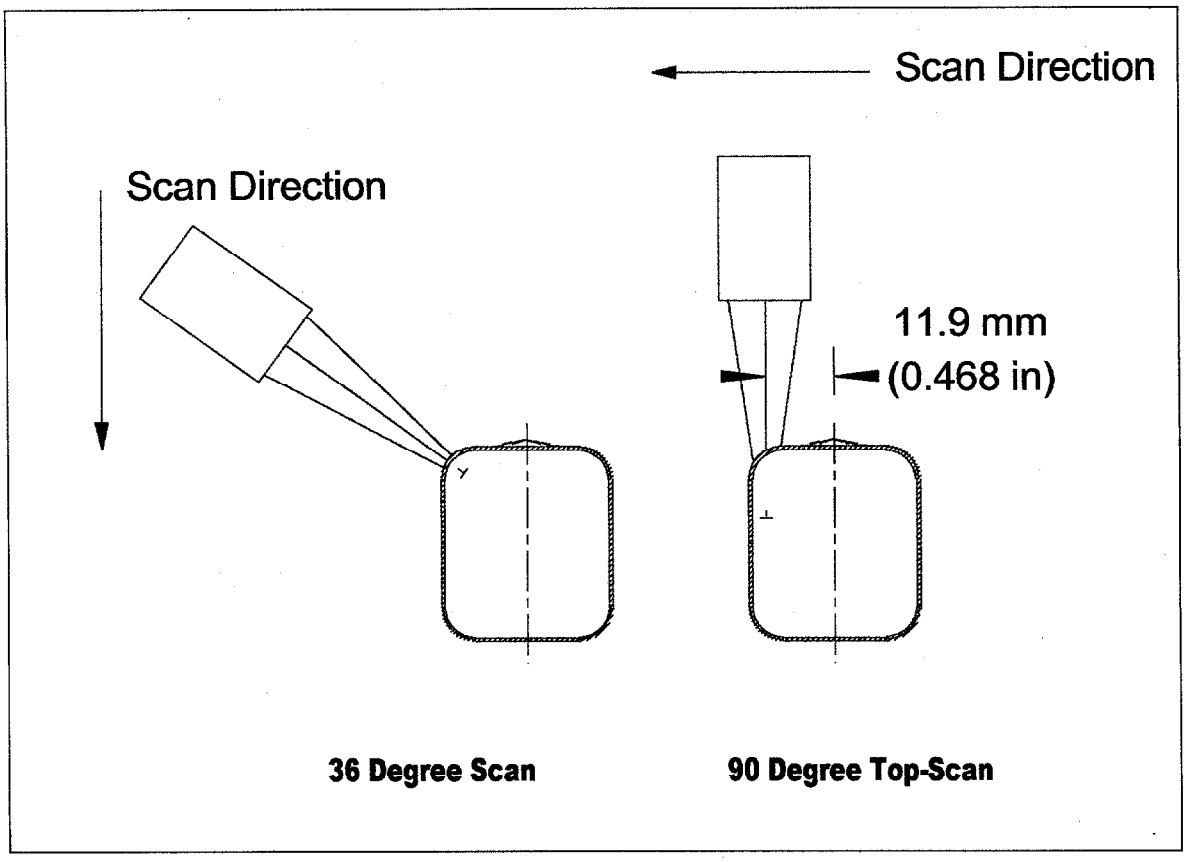

Figure 3 - Setup for 36-degree and 90-degree Lamb Wave Scans of GPHS Fueled Clads.

The setup was modified so that the sound was incident on the knuckle of the capsule along an axis that is parallel to the capsule axis. This scan mode is referred to as a Top Scan. In this scan mode, the transducer is scanned along the X-axis (horizontal axis in the plane that contains the capsule axis). This scan mode is shown on the right side of Figure 3. This mode has a narrow region where Lamb waves are generated.

In order to understand the signals that are generated in the capsule wall, it is necessary to understand the different Lamb wave modes that can be generated. Lamb waves are a form of elastic, guided wave propagation. Because Lamb waves are dispersive (both phase and group velocities are functions of frequency), understanding their behavior is important. In plates with a thickness on the order of a wavelength, elastic wave modes are generated that are analogous to the transverse electric (TE) and transverse magnetic (TM) modes of electromagnetic waves in waveguides. When measurements are being made in the time domain, the behavior of the group velocity is of interest because that velocity is the quantity that is measured. As in the case of electromagnetic wave propagation, the group velocity of Lamb waves may either exceed (normal dispersion) or be less than (anomalous dispersion) the phase velocity.

W. A. Simpson of the Oak Ridge National Laboratory (ORNL) studied the propagation of Lamb waves in iridium. Strictly speaking, the waves excited in the inspection of iridium alloy capsules are leaky Lamb waves, and the properties of such waves can be quite different from those of the true (nonleaky) Lamb wave. However, when the acoustic impedance of the material in which the waves propagate differs widely from that of the surrounding medium, the difference between a guided wave and a leaky wave is negligible.

In a given sample configuration, two classes of Lamb waves can be generated. These classes are designated as symmetric and antisymmetric modes because of the distortions induced in the plate as the wave propagates. Figure 4 is a schematic of both the symmetric and the antisymmetric Lamb wave modes. The mode of Lamb wave generated depends upon the angle of incidence, the plate thickness, and the frequency of sound.

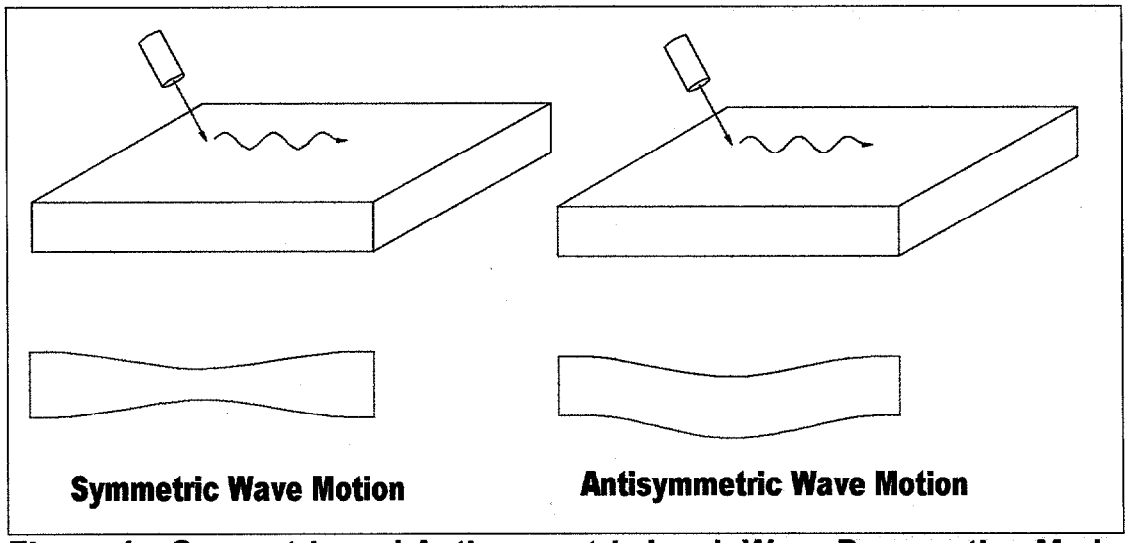

Figure 4 – Symmetric and Antisymmetric Lamb Wave Propagation Modes

Phase and group velocity curves can be calculated for a given material. A set of velocity dispersion curves are generally represented by a set of alternating symmetric (S) and antisymmetric (A) Lamb wave modes. Figure 5 shows the curves for the first four Lamb wave modes for the group velocity calculated for iridium alloy sheet. The ordinate of the graph gives the group velocity (C) of the Lamb wave normalized to that of a shear wave in iridium alloy. The abscissa is the ratio of frequency times the layer half-thickness to the shear velocity or just the half-thickness normalized to the wavelength of a shear wave in the iridium. Both axes are thus dimensionless and can be used for any thickness of iridium. The velocity of the Lamb wave generated depends upon the conditions used to generate the wave. For a given angle of incidence, several different Lamb wave modes, each with a different velocity and frequency, can be generated simultaneously.

For the Top Scan inspection geometry, three Lamb wave modes have been identified; A0, A1, and S1. These three modes generate three waves with three different velocities. The modes are identified by measuring the velocity and frequency of reflections from a slot in the standard. The three modes are superimposed on the group velocity curves in Figure 5. The first signal received corresponds to the A1 mode, the second to the A0 mode and the third to the S1 mode. The first signal is sufficiently separated from the other two Lamb wave modes so that it does not interfere with them and can be used to detect flaws in the weld.

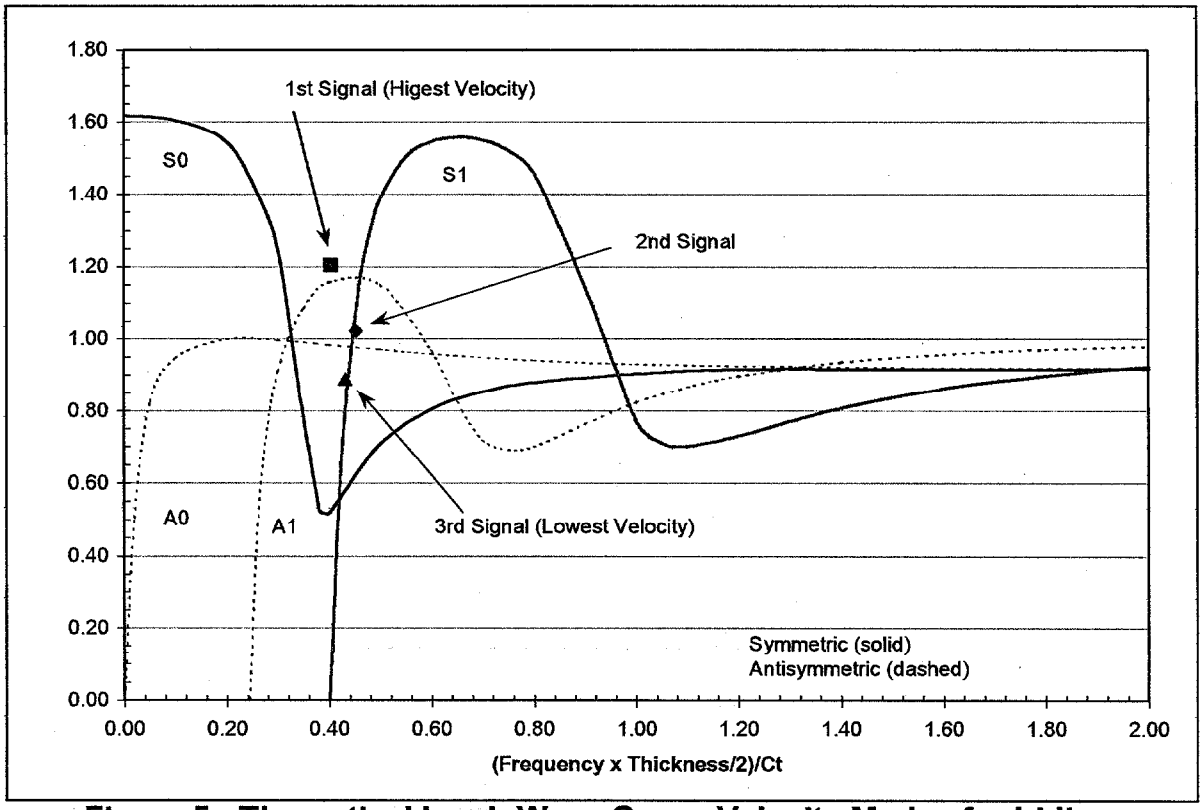

Figure 5 - Theoretical Lamb Wave Group Velocity Modes for Iridium

Figure 6 shows the ultrasonic waveforms of Lamb waves reflected from an electro-discharge machined slot. The three modes identified in Figure 5 are labeled in the plot.

It should be noted that Lamb waves will reflect from several types of conditions. A signal will be reflected from internal reflectors such as cracks, porosity, or lack-of-penetration. Signals can also be reflected from abrupt thickness changes such as suckback, weld protrusion, and capsule wall mismatch. The size of the reflection depends upon the amount of thickness change and the abruptness. A smooth change in thickness will produce a much smaller reflection than a sharp one. For weld shield fusion, the reflection comes from the side of the weld where it penetrates into the weld shield. The size of the reflection depends upon the gap between the capsule wall and the weld shield.

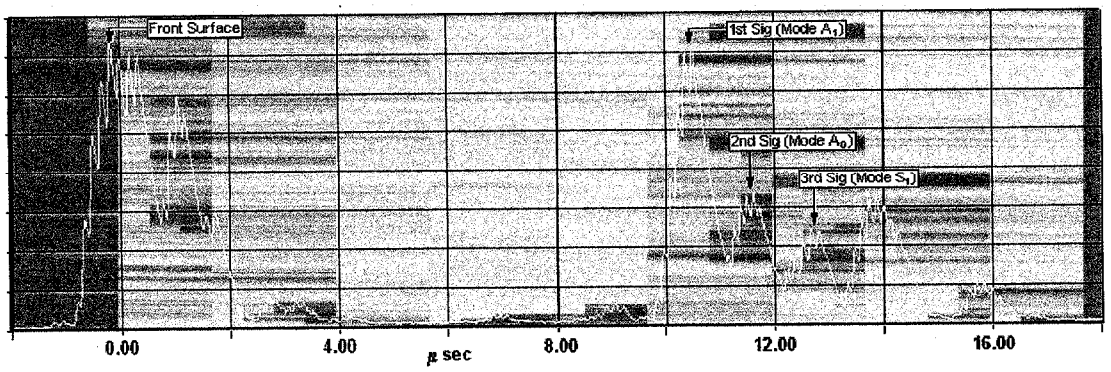

Figure 6 - Rectified Top Scan Waveform from Artifact

As the Lamb wave travels down the wall, it is attenuated. Initially, the standards were designed for the Galileo/Ulysses-type inspection with the beam incident at 32.15 degrees on the capsule cylindrical wall near the weld (Figure 2). The reference slots were placed 0.150 in. above the weld centerline so that both the top and the bottom scans could use the slots without interference from the weld. For the Top-Scan (Figure 3), reference slots 0.150 in. above the weld centerline might not give an adequate calibration, so slots were placed just above the top edge of the weld. In addition, one slot was added just below the weld and one slot was added in the center of the weld to enable the gate to be set properly.

The Top-Scan simplified the fueled clad inspection and gave more consistent results from standards and test CVS's. In addition, the location of a reflector with respect to the weld centerline could be determined. Figure 7 shows both the amplitude and the time-of-flight scans from a standard. Both the amplitude of the three slots used for calibration and the colorbar have been converted to equivalent size using a least-squares fit of flaw size to signal amplitude. The plot on the right is the time-of-flight plot. It too has been scaled to engineering units by converting the time to distance from the weld centerline. One can see the distance from the weld centerline of the three calibration reference slots at 285, 315, and 345 degrees, the weld centerline slot at 210 degrees and the slot below the weld at 255 degrees.

With the Top Scan, the transducer scans past the knuckle along the X-axis. There is only a very small range of positions that exist where the incident angle to the surface of the capsule is appropriate to generate Lamb waves. Thus the time to the incident surface and the position of the entry point do not change during the scan as they did for the 36-degree scan.

The initial investigation of the Top-Scan indicated that the center frequencies of the Lamb waves that were generated were between 3.6 and 4.2 MHz. Thus, a 3.5-MHz transducer was used for the inspection.

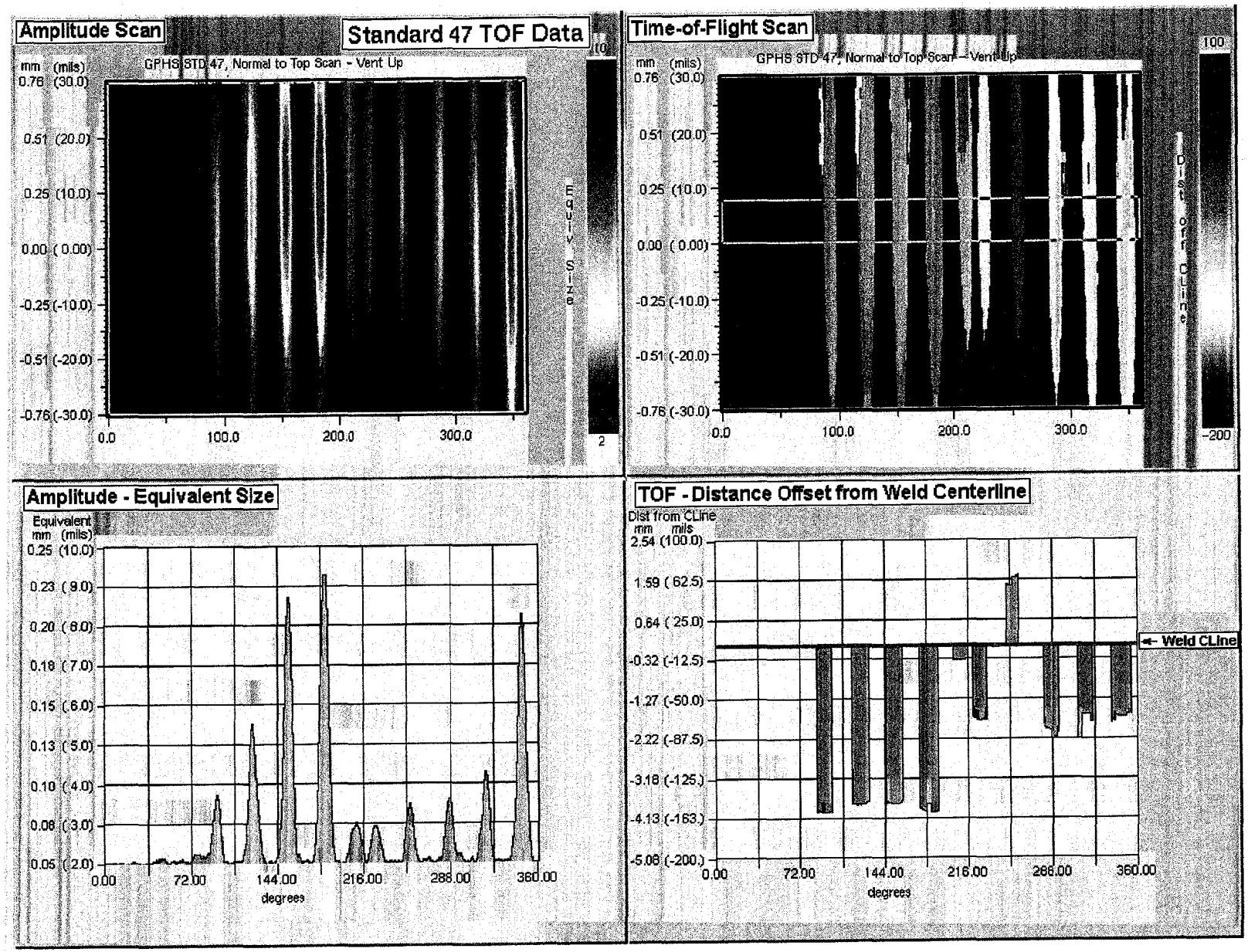

Figure 7 - Top-Scan Amplitude and Time-of-Flight Data from Standard

Top-Scan Inspection Qualification

To qualify the Top Scan inspection technique, data were taken from each of four standards and from a series of test CVS's that were used in a round robin experiment at Y-12, LANL and WSRC. The data were used to determine the differences between standards and the repeatability of different systems on the same parts using different standards for calibration.

Calibration curves were obtained based on ultrasonic measurements of three specific slots in each standard. The average standard deviation of the responses over the four calibrations was 6.4 μm (0.00025 in.) and is a measure of the repeatability of the calibration.

In order to qualify the Top Scan, eleven GPHS CVS's were inspected at WSRC, LANL, and Y-12 using the Top-Scan inspection technique and the standards. The data from these CVS's have been useful in verifying the sensitivity of the Top-Scan to a variety of weld conditions and in the development of the time-of-flight analysis of the Top-Scan data. One of the CVS was made using a new weld shield design which does not require weld tabs. The remaining CVS's were made using old hardware with weld shields that required weld tabs.

The CVS's were cut open at one end so that the weld shield could be removed and the quality of the weld root could be inspected visually. Thus, the Top-Scan weld inspection could be made only from the closed end of the CVS. The CVS's contained a variety of conditions including weld shield fusion, suckback, weld tabs, and small defects near the weld overlap area.

Each of the CVS's was inspected using the GPHS inspection acquiring amplitude and time-of-flight data. The gate was set to detect signals within 3.8 mm (0.150 in.) of the weld centerline.

The CVS's were inspected at WSRC using dye penetrant. Three of the CVS's had dye penetrant indications. Examination of replicas of the indications showed small cracks in the area of the dye penetrant indications.

One of the CVS's not only contained suckback and weld shield fusion but also contained a short area where the weld root was not visible on the ID surface of the CVS. This area is identified as lack of penetration. Figure 8 shows the amplitude and time-of-flight signals from this CVS. The area of suckback can be seen in the amplitude signal extending from 350 to 30 degrees.

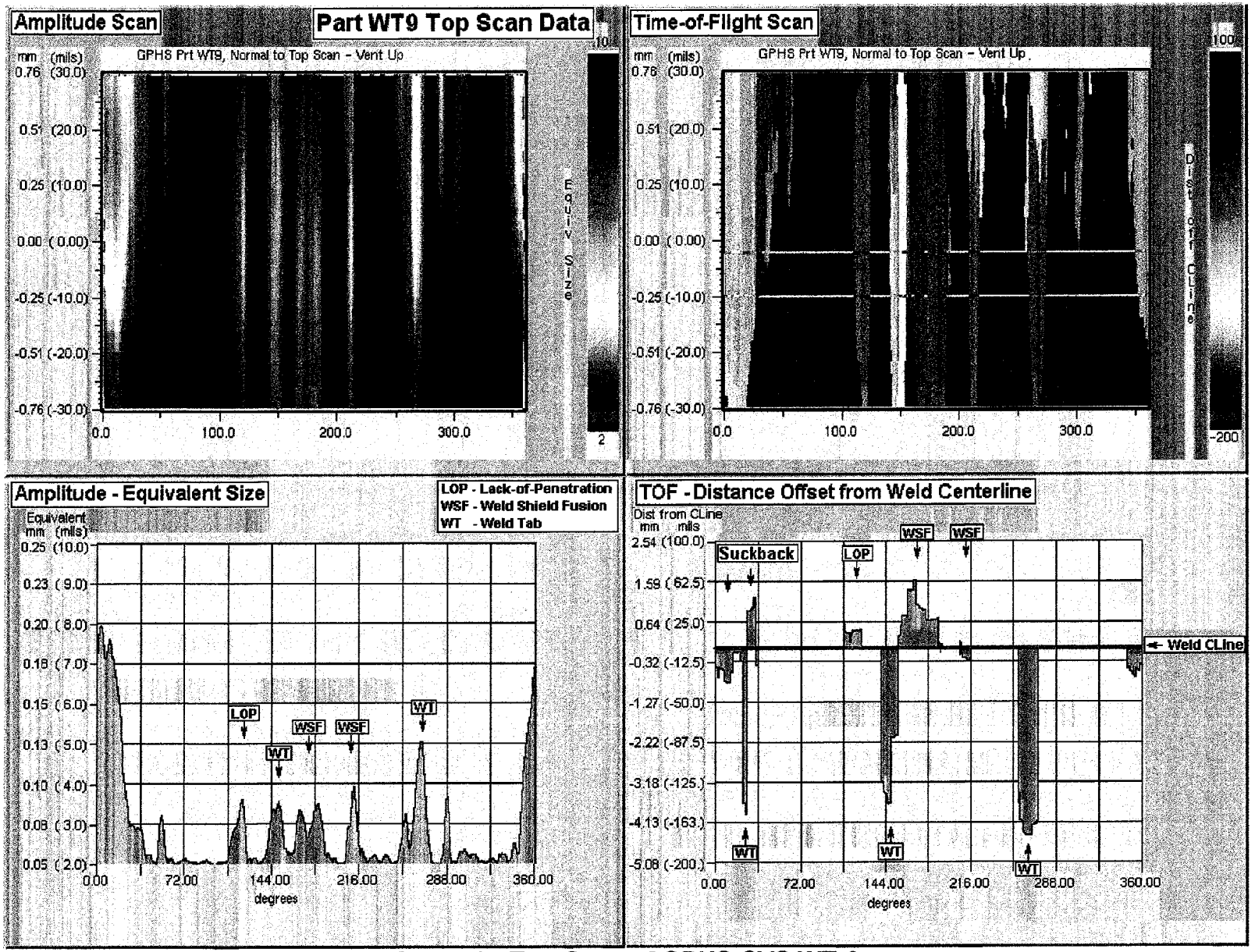

Figure 8 - Top-Scan of GPHS CVS WT-9

The weld tab signals are located at 25, 145, and 265 degrees. Although the weld tab signal at 25 degrees is masked by the suckback signal, the time of flight indicates an area near 25 degrees that appears as a dark red spot in the time-of-flight scan. The other two weld tabs can also be seen as red indications. The time-of-flight graph in the lower right quadrant of Figure 8 indicates that these signals are located between 4.0 and 5.0 mm (~0.18 in.) below the weld centerline.

The lack-of-penetration signal is seen between 112 and 125 degrees. The time-of-flight graph shows this signal to be near the weld centerline. The long section of weld shield fusion between 170 and 185 degrees is located approximately 1 mm (0.04 in.) above the weld centerline while the small spot of weld shield fusion at 216 degrees is near the weld centerline.

Figure 9 is a photograph of the replica taken from the ID surface of WT-9. The amplitude scan of WT-9 gives no indication of the source of the detected signal. The time-of-flight scan can shed some light upon the distance along the CVS wall from the weld centerline to the detected signal.

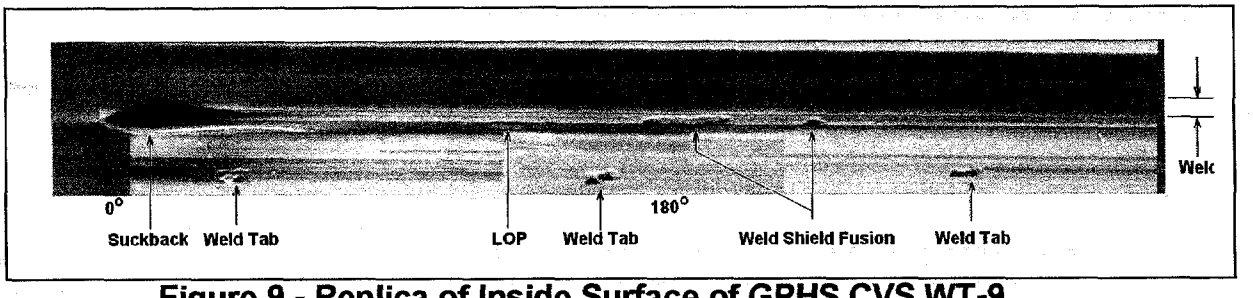

Figure 9 - Replica of Inside Surface of GPHS CVS WT-9

Signals near the weld centerline that exceed the reject threshold will have to be considered as detrimental to the fueled clad. However, the time-of-flight scan can identify signals that are at the edge of the weld. Signals at the edge of the weld are generally caused by geometric effects such as the edge of suckback and are not detrimental to the fueled clad. The ability to identify weld-shield fusion will depend upon the width of the weld fusion. The greater the distance from the weld centerline to the edge of the weld shield fusion, the easier the detection of weld-shield fusion.

Limitations

Weld defects are normally defined as conditions that reduce the cross-sectional area of the weld. There are five conditions that have been identified as detrimental to the fueled clad weld and are shown in Figure 10. Centerline root cracks, internal cracks and lack-of-fusion/penetration produce a severe stress concentration.

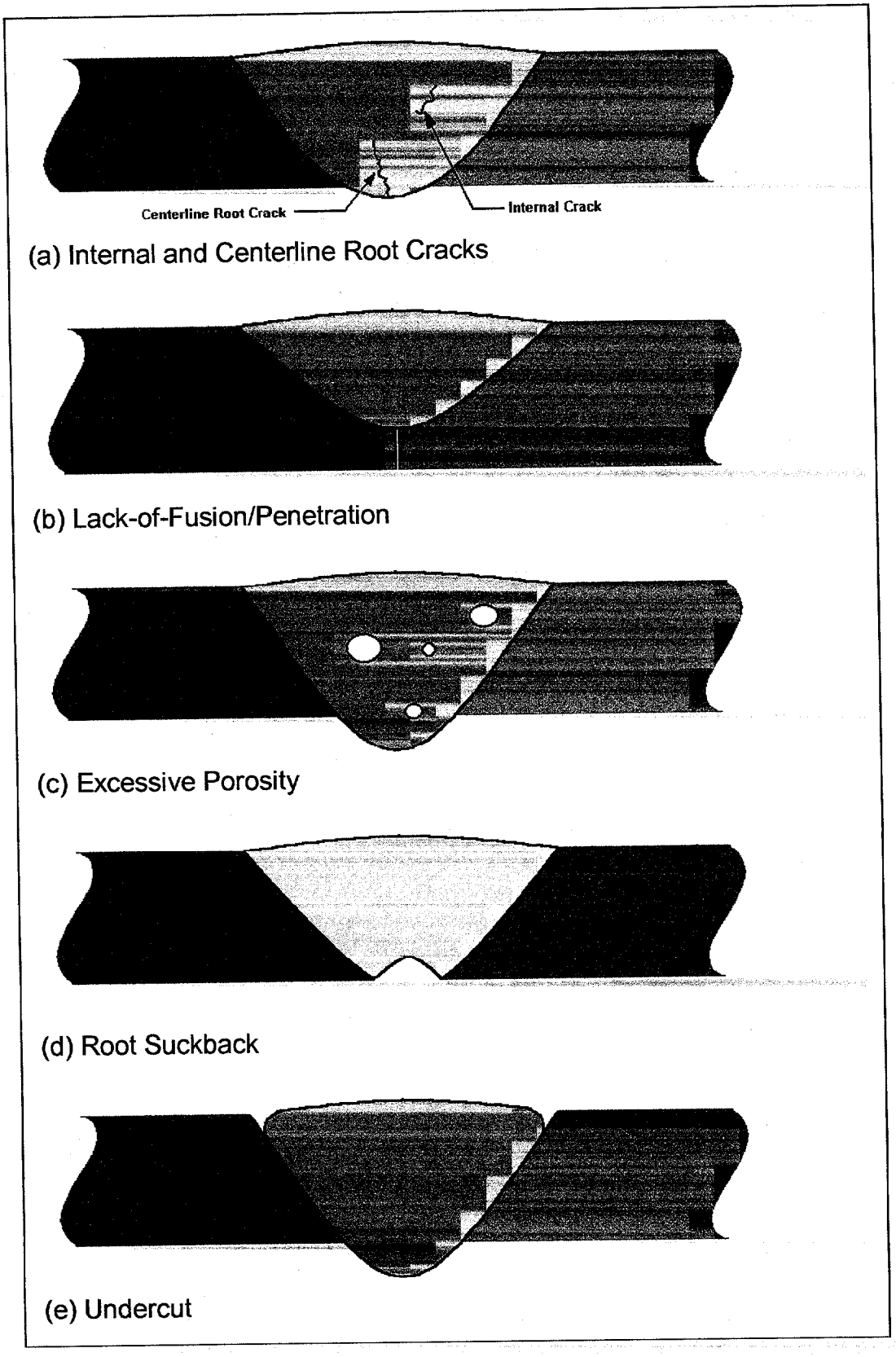

Figure 10 - Detrimental Weld Defects

Excessive porosity does not produce as severe a stress concentration but is detrimental above a certain size for a single void or concentration for multiple voids. Weld root suckback can compromise the weld load-carrying ability and undercut produces an OD surface stress concentration but is detected by visual inspection and rarely found.

As experience was gained in inspecting CVS's, it was found that there were some benign conditions that produced ultrasonic signals with amplitudes that were of the same magnitude as that received from a defect. These conditions, shown in Figure 11 include weld shield fusion, internal mismatch and internal concavity (or suckback) coupled with an external bulge. A study[6] of ultrasonic results from the production welds documented some of these conditions. The time-of-flight analysis of the Top Scan data was unable to unambiguously identify these conditions.

One problem was that the Top Scan recorded only the amplitude and time to peak signal of the gated area of the scan. As indicated in Figure 5, the lamb wave inspection produces three different lamb waves with different velocities. It was found that in some situations, the largest signal was the second signal instead of the first. This produces unreliable time-of-flight data.

In order to improve the ability of the system to record and analyze data, the data acquisition system was modified to acquire full waveforms for analysis. From this data, a B-scan analysis technique was developed.

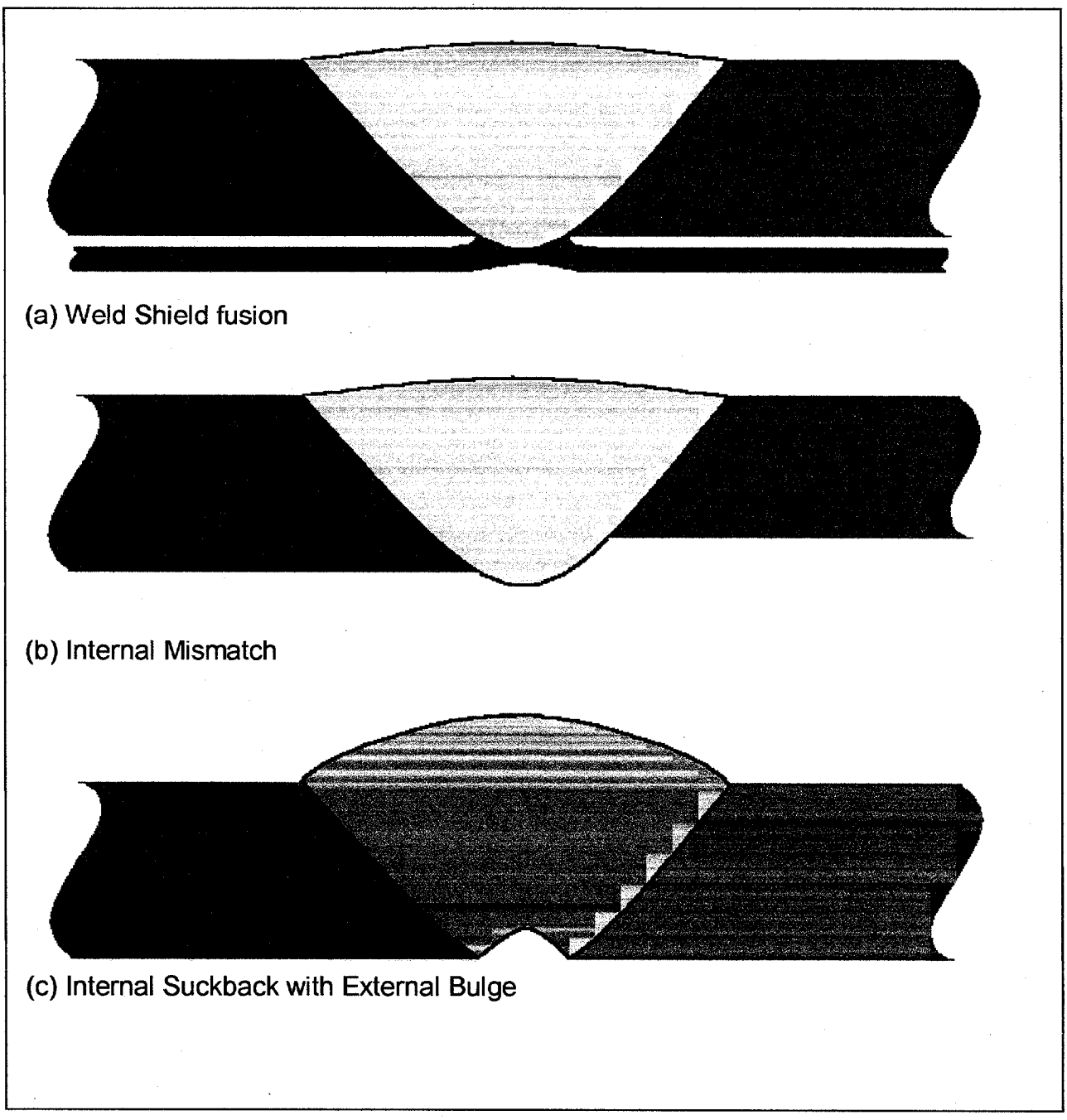

Figure 11 - Benign Geometric Anomalies

DEVELOPMENT OF B-SCAN INSPECTION

The Top Scan inspection using amplitude and time-of-flight data was usually sufficient to certify the weld quality. As mentioned before, a threshold was set for a "number 8" flaw which was determined to be equivalent to a 0.132 mm (0.0052 in.) slot in the standard. If a fueled clad had no indications that were above the threshold, the weld was judged to be sound. Only when signals were detected above the threshold was it necessary to acquire additional data. The type of data obtained from a time-of-flight scan is shown in Figures 7 and 8.

For the B-scan inspection, the index axis of the scan was adjusted for the maximum signal and a single RF waveform scan consisting of 360 waveforms was taken as the fueled clad was rotated about its axis. The bipolar RF waveform data was rectified to produce a unipolar video waveform before data acquisition. Waveform data were acquired from both sides of the fueled clad. Vent Up and Vent Down scans refer to scans with the vent cap towards or away from the transducer. Waveform data were taken only from fueled clads with indications above the threshold because the data sets were roughly 10 times the size of the amplitude/time-of-flight data sets. An example B-scan is shown in Figure 12. The vertical axis is the scan axis, which is the angular position of the fueled clad. The horizontal axis is the time of the waveform. Two example waveforms are shown which represent the data at 127 and 305 degrees. The schematic shows that the signal enters the fueled clad at the top surface and is reflected from the weld in areas where there are defect or geometric conditions. The waveform amplitude is displayed as color that is calibrated in engineering units.

B-scan data as well as amplitude and time-of-flight data were received from LANL for 29 fueled clads that were welded at LANL. All of the fueled clads had at least one area where the ultrasonic signal was large enough to cause the fueled clad to be classified as nonconforming.

During this initial phase of inspection it became evident that there were several benign conditions such as weld shield fusion (WSF) and wall thickness mismatch that might be generating the signals which caused the fueled clads to be judged as nonconforming. The weld penetrating through the capsule wall into the weld shield causes weld shield fusion. When this condition occurs, there is a change in the weld root geometry that can cause an ultrasonic signal to be reflected from the portion of the weld root that tacks into the weld shield. The distance of the gap between the capsule wall and the weld shield will determine the amplitude of the reflection. Thus, if the weld shield is touching the capsule wall the reflection will be small, while if there is a gap between the weld shield and the capsule so that the weld protrudes across the gap to tack into the weld shield there will be a larger reflection. Add mismatch to this condition and you can have a complicated signal return. In addition, the propagation of Lamb waves is affected because the effective wall thickness of the capsule has changed. This is a benign condition even though signals greater than the reject level may be detected.

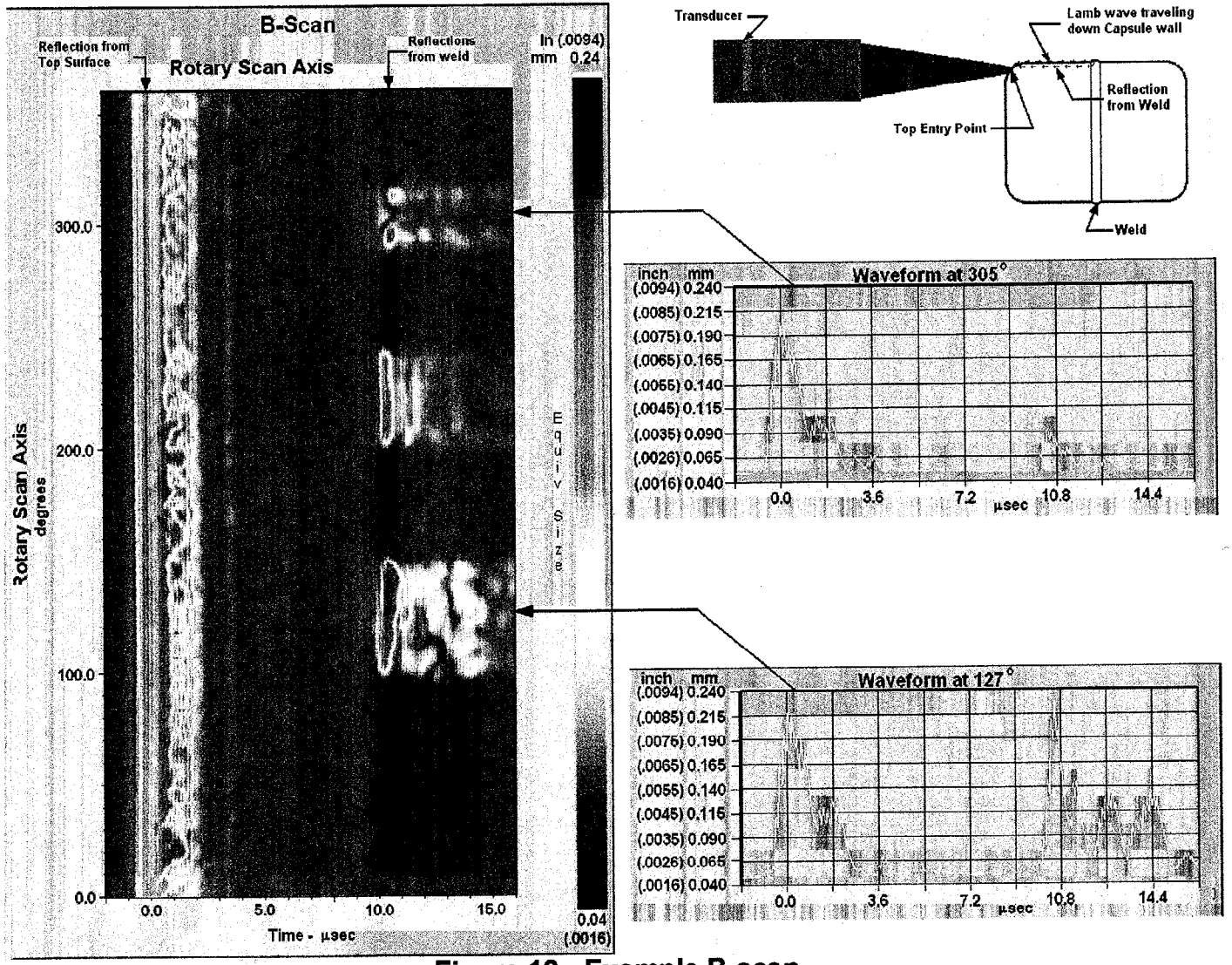

Figure 12 - Example B-scan

The standard ultrasonic inspection consists of sending a Lamb wave down the wall of the fueled clad and detecting the reflection from any interfaces in the weld. The amplitude of the signal is recorded. Signals from known size artifacts (electro-discharged machined slots) in a standard are used to calibrate the system. As mentioned earlier in this report, a time-of-flight measurement was implemented to try to detect the position of the reflecting surface that caused the signal. Since WSF should have some width, the signals from the WSF should occur away from the weld centerline.

Since the Lamb wave inspection generates several different modes of Lamb waves, each with a different velocity, several signals will be detected from a well-defined reflector. The time to the signal will depend upon the Lamb wave velocity. For a reflection from a reference slot such as the electro-discharged machined slots in the standard, the first signal received (from the highest velocity Lamb wave) is the largest. It has been observed on data received from LANL on several of the GPHS fueled clads that sometimes one of the slower Lamb waves produces the largest signal. This can cause the signal to appear to have been reflected from a point that is further from the transducer.

In order to try to identify the types of signals obtained from the different defects shown in Figure 10 and the different geometric conditions shown in Figure 11, we evaluated the B-scan data from the 29 fueled clads that had signals above the reject level.

We identified several signal types. The first category includes short signals located near the weld centerline in the weld overlap area between 10 and 30 degrees. Cracking in the weld tie-in area during production of the Galileo/Ulysses GPHS fueled clads led to the initial development of the first-generation ultrasonic test for girth weld inspection at the Savannah River Plant. It was found that this cracking was caused by the low melting Ir_5Th eutectic at the weld centerline. In the area of the overlap where the second weld pass is less than fully penetrated (as the weld current is reduced at the end of the weld), grain boundary separation occurs under the influence of thermal and mechanical stresses[6]. This can produce weld cracking (Figure 10a). Figure 13 shows this type of response from a 60-degree section of the weld overlap region from fueled clad FC0024. Five plots are shown in Figure 13. The first plot shows the peak amplitude of the signal in the gate, converted to engineering units. The second plot shows the time-of-flight to the peak, scaled to distance from the weld centerline. The third plot is the B-scan. The horizontal axis is the time in microseconds from the entry point at the knuckle in the fueled clad. This point and the weld centerline are labeled in the plot. The forth plot shows an amplitude graph taken from the data in the first plot. The last graph is the time-of-flight data taken from the second plot.

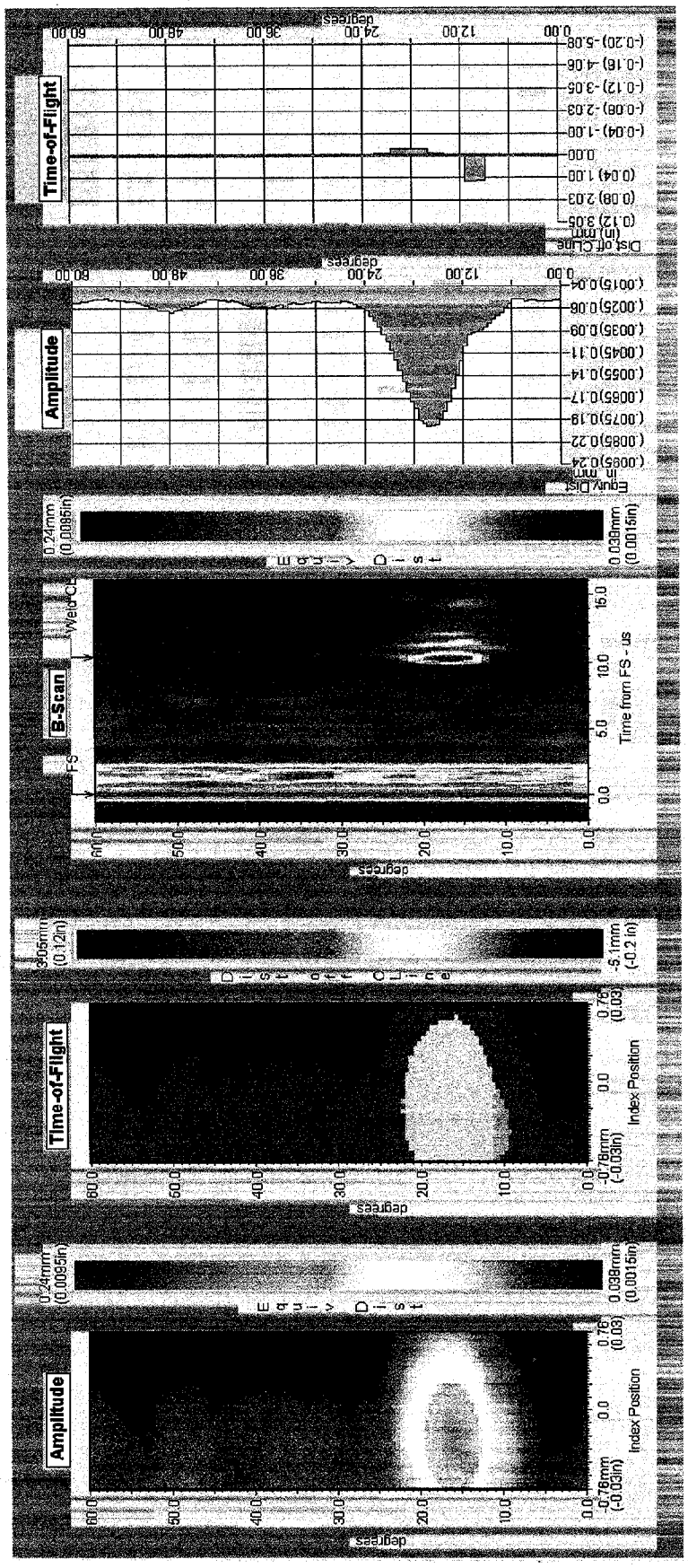

Figure 13 - Data from a Crack-like Indication in the Weld Overlap Region

Note that a positive distance from the weld centerline is later in time so the area near 10 degrees is from the second reflection seen in the B-scan. Although this fueled clad was sectioned and examined with metallography, no evidence of a crack was found. The difficulty of locating a small indication on a metallographic section may explain the inconclusive result.

The second category of signals was obtained from an area of weld root suckback with or without an external weld bulge (Figure 10d or Figure 11c). This condition occurs in the weld overlap region because the weld seals the vent grooves and internal pressure within the fueled clad causes the weld to bulge with corresponding suckback at the back of the weld. The size of the signal and the time to the signal depend upon the sharpness of the corner at the edge of the weld. Figure 8 shows the amplitude and time-of-flight data from test CVS WT9. This is a Galileo/Ulyssis type of CVS that has weld tabs. The weld shield in the Cassini fueled clads did not have weld tabs. Figure 14 shows the B-scan. For this condition, there is normally a large signal in the area of the suckback. The time varies because there are areas where the far side signal is larger than the near side signal. Also, there is a weld tab that masks a portion of the signal. Generally, suckback can be identified because there is some weld protrusion on the outside surface of the fueled clad weld. However, it is difficult to tell if there is a crack in the weld overlap region that is masked by the suckback. The amount of suckback and protrusion found in CVS WT9 is larger than that which would be accepted in a flight quality fueled clad. Typical weld protrusion/suckback signals are shown later in this report in Figures 17 and 21 for fueled clads FC0005 and FC0212.

The third category is porosity (Figure 10c). A signal would be obtained only if the porosity occupied a significant percentage of the wall thickness. Generally, large pores would produce short sharp signals. Although porosity has been detected by tangential radiography in fueled clad FC0208, it was too small to be detected with ultrasonics.

The next category consists of a rather long uniform signal. The data from most of the fueled clads (25 of 29) fall into this category. In general the first signal originates from near the weld centerline and is followed by several roughly parallel signals. The signals that follow the first signal are from different Lamb wave modes that have slower velocities. In some of the cases, the first signal is the largest from one side of the weld, while the second or third signal may be larger when inspected from the opposite side of the weld. When the second or third signal is larger, a false time-of-flight distance is measured since the system detects the largest signal in the gate. The long uniform signals are from a geometric reflector such as mismatch on the weld inside surface (Figure 11b). An example is shown for Fueled clad FC0041 in Figure 15 for the Vent Up data and in Figure 16 for the Vent Down data.

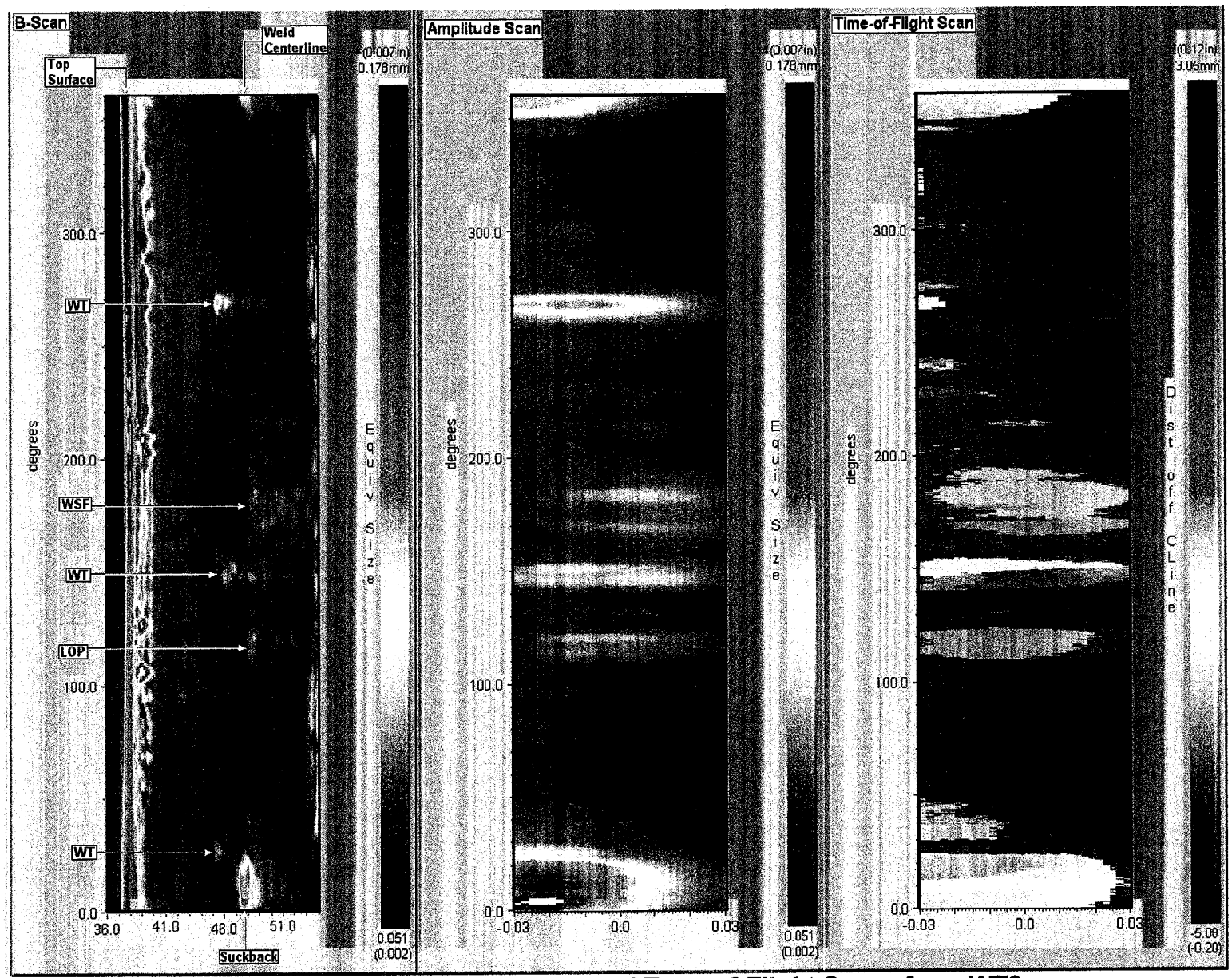

Figure 14 - B-Scan, Amplitude, and Time-of-Flight Scans from WT9

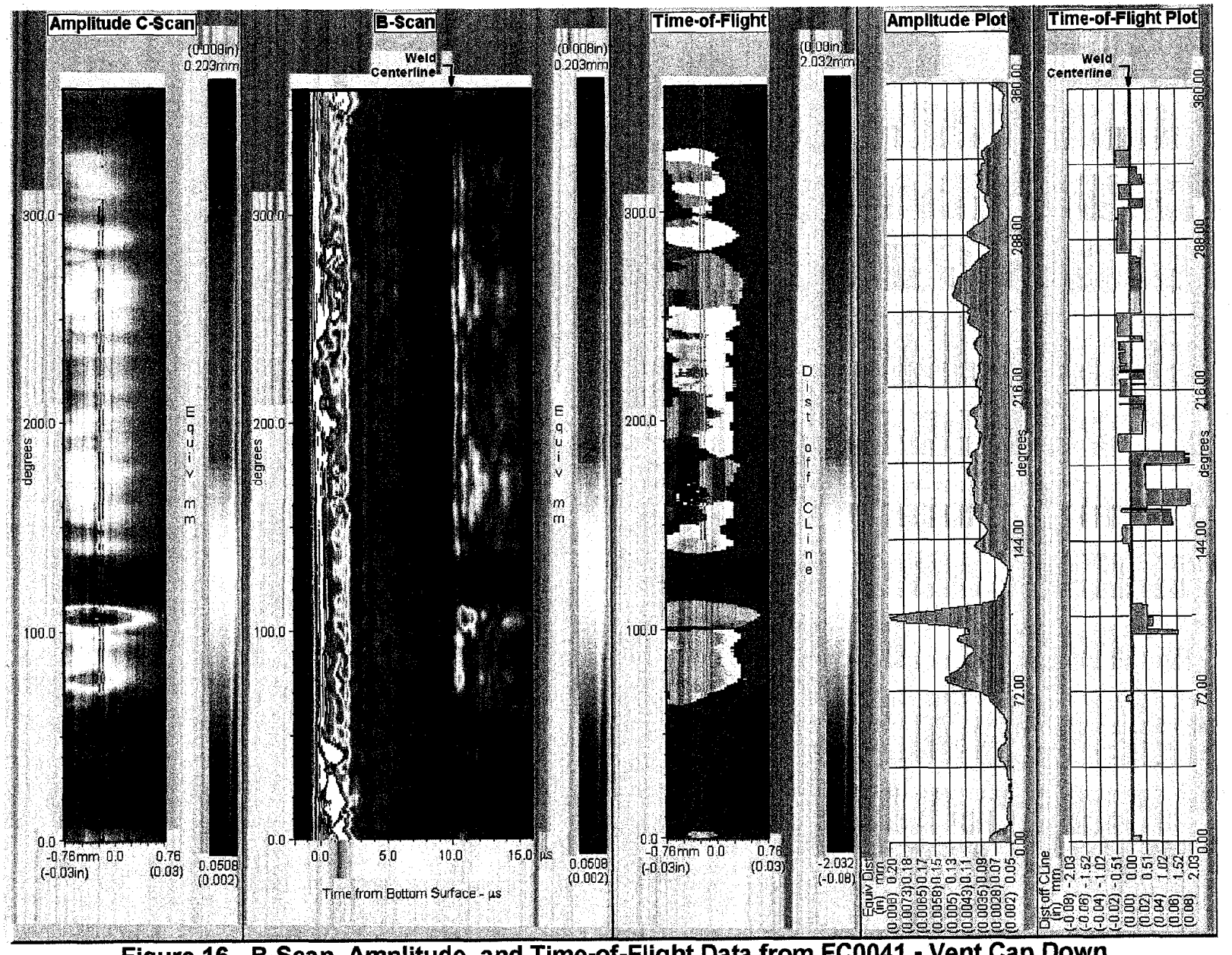

Figure 16 - B-Scan, Amplitude, and Time-of-Flight Data from FC0041 - Vent Cap Down

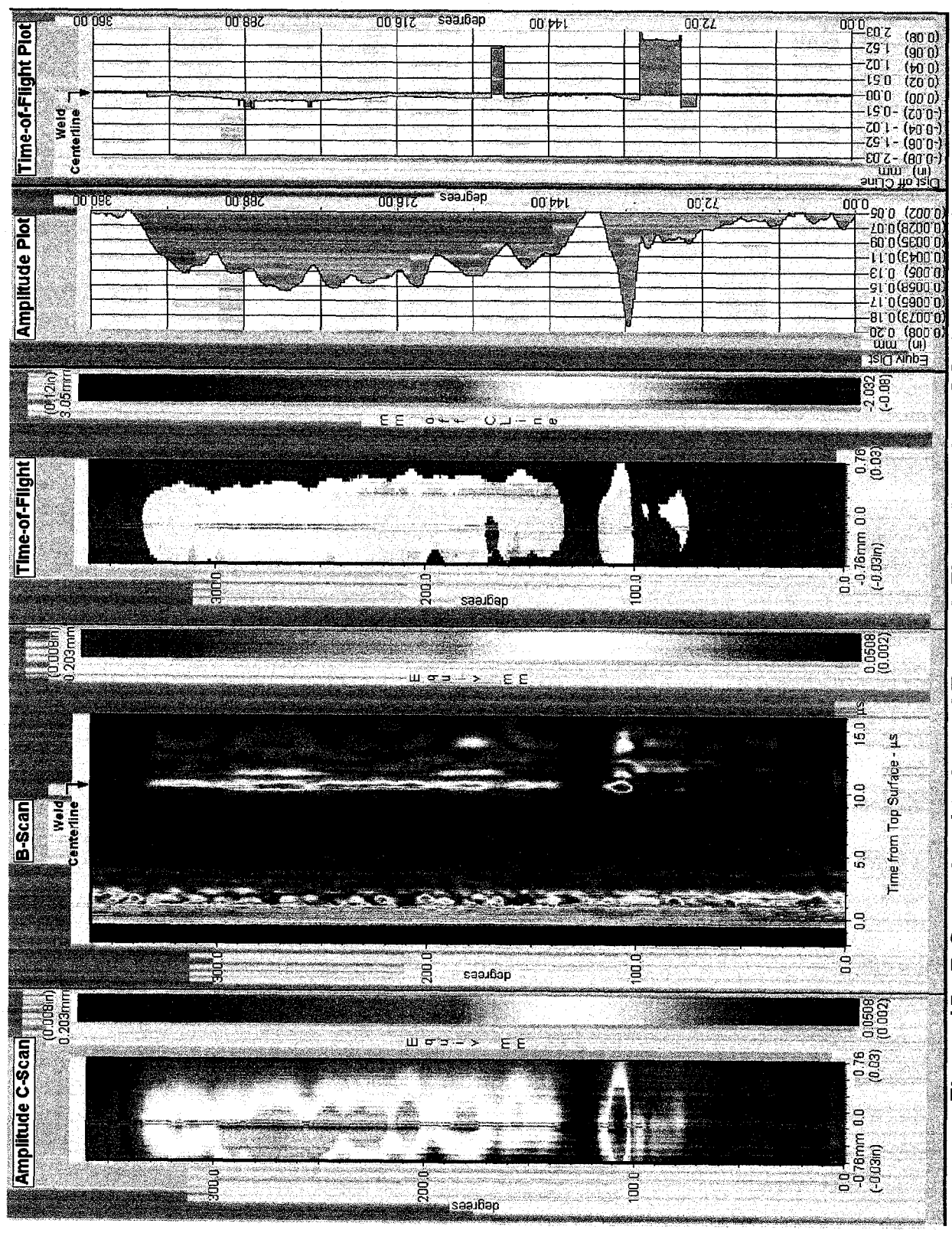

Figure 15 - B-Scan, Amplitude, and Time-of- Flight Data from FC0041 - Vent Cap Up

Other conditions could also show a long linear indication. A long section of WSF would cause a long linear indication. However, the capsule wall mismatch signal is distinctly different from WSF. It is extremely doubtful that a crack could cause this type of response because a crack would be rough and if it extended the length of these indications it would break through the capsule wall. It is also possible that a long linear signal could be caused by lack-of-penetration. With the automatic welding it is doubtful that the weld current would drop enough to cause a long section of lack-of-penetration. However, it is recommended that tangential radiography be used to identify the mismatch condition and confirm that the signal is not caused by lack-of-penetration. It might also be possible in future programs to use a normal ultrasonic inspection to identify the capsule wall mismatch.

In fueled clad FC0041 the first signal is larger when the fueled clad is inspected with the Vent Up (Figure 15). When inspected with the Vent Down (Figure 16) the second or third signal is larger. The reflection coefficient of the mismatch is different for different Lamb modes (symmetric and antisymmetric), particularly when you compare the reflection of a step increase in wall thickness with a step decrease in wall thickness.

When we have the condition where the inspection from one side of the weld produces a large first signal and the inspection from the other side of the weld produces a smaller signal the time-of-flight data does a poor job of locating the position of the reflecting surface. In Figure 16 (Vent Down) there are areas that the second signal is larger than the first. Thus, if you compare the time-of-flight data for the Vent Up (Figure 15) and Vent Down scans, the Vent Up data shows a uniform time-of-flight while the Vent Down time-of-flight data jumps back and forth between the first and second signals. Thus, it is difficult to determine the location of the reflecting surface from the time-of-flight data. In the B-scan data it is clear.

We also observe in fueled clads FC0041 a larger signal (bright spot) at the end of an area of mismatch (110 degrees for both the Vent Up and Vent Down scans). This can occur at a sharp corner where the corner absorbs the energy and then reradiates it as a point source. This would indicate that there was a sharp change in the geometry at the end of the mismatch, perhaps caused by a short section of WSF.

The cups used to fabricate the fueled clads have wall thickness variations that are aligned at zero and ninety degrees due to the rolling variations in the sheet that is used to form the cups. When a fueled clad is fabricated, the two cups are rotated 90 degrees to offset the thickness variations and give the capsule a constant average wall thickness. Since the fixturing aligns the OD of the cups, all the wall thickness variations are forced to the fueled clad ID. This is the cause of the mismatch.

In Figure 5, the velocity of first and second signals does not change appreciably with wall thickness change. However, the slope of the plot of the third signal (S_1) is steep indicating that there is a significant velocity change with wall thickness change. This can be seen in Figure 15. In the B-scan plot between 190 and 260 degrees the time (horizontal position) of the last signal (right side of the plot) changes significantly. It looks like a "C." The effect is also seen between 200 and 240 degrees. This demonstrates the

variation in cup wall thickness and is conformation of fueled clad wall thickness variations.

The amplitude of the signal obtained from mismatch depends upon the sharpness of the step between the two wall thicknesses. A weld that barely penetrates the wall may not wipe out the sharp corner of the thicker cup. A wider weld bead on the inner contour will produce a smooth transition between the two wall thicknesses and thus a smaller signal. After the completion of initial analysis of the first 18 fueled clads that were nonconforming with the normal ultrasonic inspection, the welding current was increased. The number of fueled clads reported after the welding current was increased was significantly reduced.

The next category is the signal from WSF (Figure 11a). The characteristic response from WSF is a mottled appearance in the B-scan. Where there is a long section of WSF, this condition is rather easy to identify, but where the WSF is short it is more difficult to identify. An example of WSF is shown in Figure 14 for CVS WT9. There is a section of WSF identified at 180 degrees.

The B-scan coupled with the time-of-flight measurement and tangential radiography should enable an engineer to judge if a signal is from a benign or actual defect.

When a part or standard is mounted for inspection, the top surface may be tilted. Therefore, the distance from the transducer to the part surface can change as the part is rotated during inspection. Runout of this type can produce typical errors of 25 mils. The weld is 100 mils wide, so this amount of error is significant. In addition, runout of the standard can produce calibration errors that are multiplied by the runout of the part.

We have incorporated an algorithm that corrects for runout errors. Calculations are based on minimum and maximum water path values for part and standard, where water path corresponds to the distance from the transducer to the part surface. The minimum and maximum water path is measured when the part is mounted and then the time-of-flight data is corrected for the runout. The algorithm also corrects for water path variations between the standard and the part.

PRODUCTION INSPECTION RESULTS

The nondestructive testing of the girth welds for production GPHS fueled clads involved five separate inspections[6]. The inspections in order of application are as follows:

1. Visual inspection in the welding fixture.
2. Ring gage go/no-go inspection. This sets the maximum diameter of the fueled clad and eliminates fueled clads with excessive weld protrusion.
3. Helium leak testing.
4. Ultrasonic C-scan testing using the top scan orientation. Amplitude and time-of-flight data were acquired. The rejection level was set to 0.13 mm (0.0051 in.). Two ultrasonic scans were made -- one in the Vent Up orientation and one in the Vent Down orientation. B-scan data were taken from any fueled clad that was rejected by the ultrasonic C-scan inspection.
5. Tangential radiography. Any fueled clad that was rejected by the ultrasonic C-scan inspection was inspected using tangential radiography to identify benign geometric conditions.

Of the 317 fueled clads that were fabricated, 284 were subjected to ultrasonic testing. Of these, 44 fueled clads were initially rejected by the ultrasonic C-scan test for having signals that were greater than the reference threshold from a 0.13 mm (0.0051 in.) slot. B-scan inspection was performed on 29 of these fueled clads. Table 3 summarizes both the ultrasonic amplitude and the B-scan data as well as the tangential radiography data for these 29 fueled clads

The ultrasonic data acquisition program is able to calibrate the data and convert it into engineering units. It is then able to analyze the data and determine those areas where the signal exceeds the threshold. The Ultrasonic Peak Amplitude columns in Table 3 summarize the results from the test reports for these fueled clads. The B-scan plots that are taken for nonconforming fueled clads are then evaluated by an engineer to determine if the signals have characteristics of defects or benign conditions. We were not able to automatically analyze the B-scan data. However, we followed an evaluation protocol to aid in identifying the signal conditions. The protocol is as follows:

1. First determine if there is a short signal above the threshold in the critical weld overlap region between 0 and 30 degrees. Determine if the signal is located near the weld centerline. The length of the signal is generally less than 2.5% of the circumference. If the signal does not extend beyond the peak at a lower amplitude the signal is potentially a crack. It is differentiated from protrusion/suckback by its total length. Protrusion/suckback will generally extend for a longer length at a lower amplitude.

2. Look for long linear signals. A significant portion of the signal may be below the threshold. The multiple reflections (to the right of the initial signal in the B-scan) may or may not be well defined. These signals are caused by geometric conditions such as internal mismatch or weld shield fusion. It is not always possible to discriminate between internal mismatch and weld shield fusion; however, the next two steps attempt differentiation.

3. If the second or third peak is curved then the condition is internal mismatch. There may be breaks in the signal where the thinner wall switches from one cup to the other. Look for well defined multiple reflections. The second peak may be higher than the first peak on one of the two B-scans. These areas are also generally caused by internal mismatch. Tangential radiography can confirm this condition.

4. Look for short to medium length sections that are linear. The second and third peaks may be hard to identify. In other words there will not be parallel lines behind the first peak. These sections are generally weld shield fusion. Many times there will be a larger signal at the start or end of the area of weld shield fusion.

5. Look at the maximum amplitude of the signal. The larger the maximum signal the more important it is to have indications of internal mismatch or weld shield fusion to accept the fueled clad. This is particularly true if the signal is large on both the Vent Up and the Vent Down scans, It is also important to try to verify the condition using tangential radiography.

The B-scan data are plotted in Figures 17-21. Each figure contains both the Vent Up and the Vent Down B-scans for six fueled clads (Figure 21contains data from only 5 fueled clads). As in the previous B-scans shown in this report the vertical axis is the scan (rotary) axis in degrees and the horizontal axis is the time from the front surface in microseconds. The color of the display represents the amplitude of the signal as shown from the colorbar on the right of the figure. The rotary and time axes are the same for all 12 plots in each figure. In the areas where the signal exceeds the threshold there is a blue line on the right side of the image.

Looking at Figures 17-21, several observations can be made. First of all, the location of the weld line can be seen on most of the plots. The weld line appears as a thin line at about 10 microseconds from the front surface. In Figure 17, the location of the front surface and the weld line are labeled for the Vent Up plot of FC0005. Also labeled is the critical weld overlap area.

The data can be separated into several classes using the protocol listed above. The first class is short signals that occur in the weld overlap region. There are signals in this critical region for fueled clads FC0005, FC0024, FC0049, FC0053, and FC212. The signals are above the threshold level only for fueled clads FC0024, FC0053, and FC0212. In fueled clads FC0005 and FC0212 there is some length to the signal (at a lower amplitude) indicating that these signals are probably due to protrusion/suckback. Thus, only fueled clads FC0024 and FC0053 were identified to have potential cracks and were not used. Short signals above the threshold are also seen in fueled clads FC0041, FC0062, and FC0089. None of these signals are in the critical overlap area and all are associated with a longer area of low level signal. Thus, these signals are probably due to small sharp geometric effects at the end of internal mismatch or associated with weld shield fusion.

Table 3 – Summary of Ultrasonic and Radiographic Data from LANL GPHS Fueled clads

Part Number	Run Date	Ultrasonic Peak Amplitude						Signal in Overlap	Mismatch	Curved Signal Location	Parallel Signal Location	WSF	Location of WSF	Radiography			
		Vent Up			Vent Dn									IM	ST		Comments
		Amp Mils	%>Th	Angle Deg	Amp Mils	%>Th	Angle Deg									Angle Deg	
FC0005	2/1/95	5.32	0.3%	227.0	4.13		21.0					x	200-350		x		ST @ weld
FC0024	1/20/95	3.90	0.0%	18.5	7.79	2.1%	16.5	x							x		ST wall above weld
FC0025	1/20/95	9.36 5.53 5.53	22.9%	159.5 203.0 226.5	8.50	21.7%	196.5		x	200-250	125-200				x	144 + 3 loc	ST at weld area
FC0030	1/25/95	8.12 6.56 5.62	17.9%	130.0 158.0 231.0	8.65 8.47 5.44	23.9%	134.5 179.5 100.0		x		100-190			x	x	127 131 186	Step @ 131, 186,234 (largest: 8mil) pointed tip @ 127 touching wall
FC0033	1/24/95	6.39	7.2%	301.5	5.96	3.9%	264.5		x	290-320							
FC0034	1/24/95	6.25	5.0%	276.0	6.02	3.1%	273.5		x		270-292				x		ST wall at weld area
FC0037	1/31/95	6.45 5.31 5.25	18.2%	216.0 171.5 262.0	4.74		227.5		x	135-280				x	x	174 201	Step and ST @ 174 & 201
FC0040	1/31/95	9.35 6.87 6.39 5.61	26.5%	139.5 295.5 210.5 313.0	7.68 5.97	14.4%	105.0 293.5		x	200-240 290-320	100-150			x	x	126 216 220 224	10 mil step & ST@ 126 & 290, step & ST@216, no shield contact @ 220,224
FC0041	1/31/95	7.71 6.39 6.00 5.82 5.61	23.6%	107.0 268.0 246.0 207.5 229.5	7.97 5.46	3.2%	106.5 78.0		x	130-330	70-120			x	x	108 270	step & ST @ 108 & 270
FC0045	2/1/95	5.94 5.32	5.0%	224.0 238.5	5.47	0.8%	218.0		x	215-250					x	158 162 166 220	no shield contact @ 158 & 162, ST @ 166 & 220
FC0048	1/20/95	4.64		275.5	5.26	0.3%	267.0		x	160-330					x		ST weld & capsule wall
FC0049	1/23/95	7.20 5.35	6.8%	204.5 222.5	4.67		269.0		x	190-320				x	x	205	2 mil & less porosity in cluster, step & ST
FC0050	1/27/95	5.82	1.0%	105.5	6.03	3.9%	103.0		x		105-125				x	107 124	ST near weld @ 107&124, shield overlap@124

Table 3 – (Continued)

FC0053	1/27/95	3.47		32.5	7.03	1.5%	30.5	x							x		Weld protrusion which touches shield
FC0056	2/3/95	5.32	0.7%	194.5	4.04		206.0		x	180-240				x	x	191 15	ST & step @ 191, Bulge & 18 mil suckback @15
FC0062	2/28/95	4.11		106.5	5.41	0.6%	111.5		x	110-170							
FC0065	2/3/95	5.47	0.4%	277.5	6.21 5.26	3.3%	239.5 226.5		x	200-260 290-320					x	236 240	ST at bottom of weld area
FC0071	2/7/95	6.47 5.99 5.75 5.33	7.5%	224.5 208.5 242.5 238.0	5.87	1.3%	209.5		x	240-290	210-240						
FC0076	2/8/95	5.60 5.27	3.5%	266.0 322.5	5.72 5.27	3.5%	264.5 10.0		x		260-330			x	x	280 320	slight step & ST at bottom of weld @ 320, faint step
FC0080	2/28/95	9.42 6.63	11.5%	240.5 295.5	6.02 5.88 5.67 5.50	8.9%	273.5 231.5 250.5 299.0		x	220-310				x		243 247	Top cup thinner
FC0081	2/28/95	5.44	0.7%	353.5	5.67	1.1%	286.5		x	260-290							
FC0089	3/3/95	3.56		177.0	5.29	0.1%	83.5					x	10-100 140-200				
FC0134	6/8/95	3.97		131.0	9.52 5.8	5.8%	137.5 114.5					x	22-150				
FC0149	7/11/95	3.86		191.0	9.50 6.26	6.3%	84.0 159.5		x		75-95	x	15-300				
FC0182	8/30/95	6.85	1.4%	135.0	4.27		102.5					x	15-140				
FC0188	9/13/95	5.06		312.5	9.10 8.90 5.48	12.1%	287.0 271.5 278.0		x		200-250						
FC0197	9/26/95	6.36 5.91	6.0%	320.5 341.0	7.66 6.56	7.8%	295.5 309.5		x		280-350						
FC0208	12/12/95	9.31 9.05 5.99	20.3%	70.5 135.0 93.0	7.79 5.76 5.39 5.39 5.33	6.8%	133.0 115.0 57.0 49.0 73.5		x		110-135	x	150-330				
FC0212	12/18/95	6.12	1.5%	18.0	4.42		36.0										

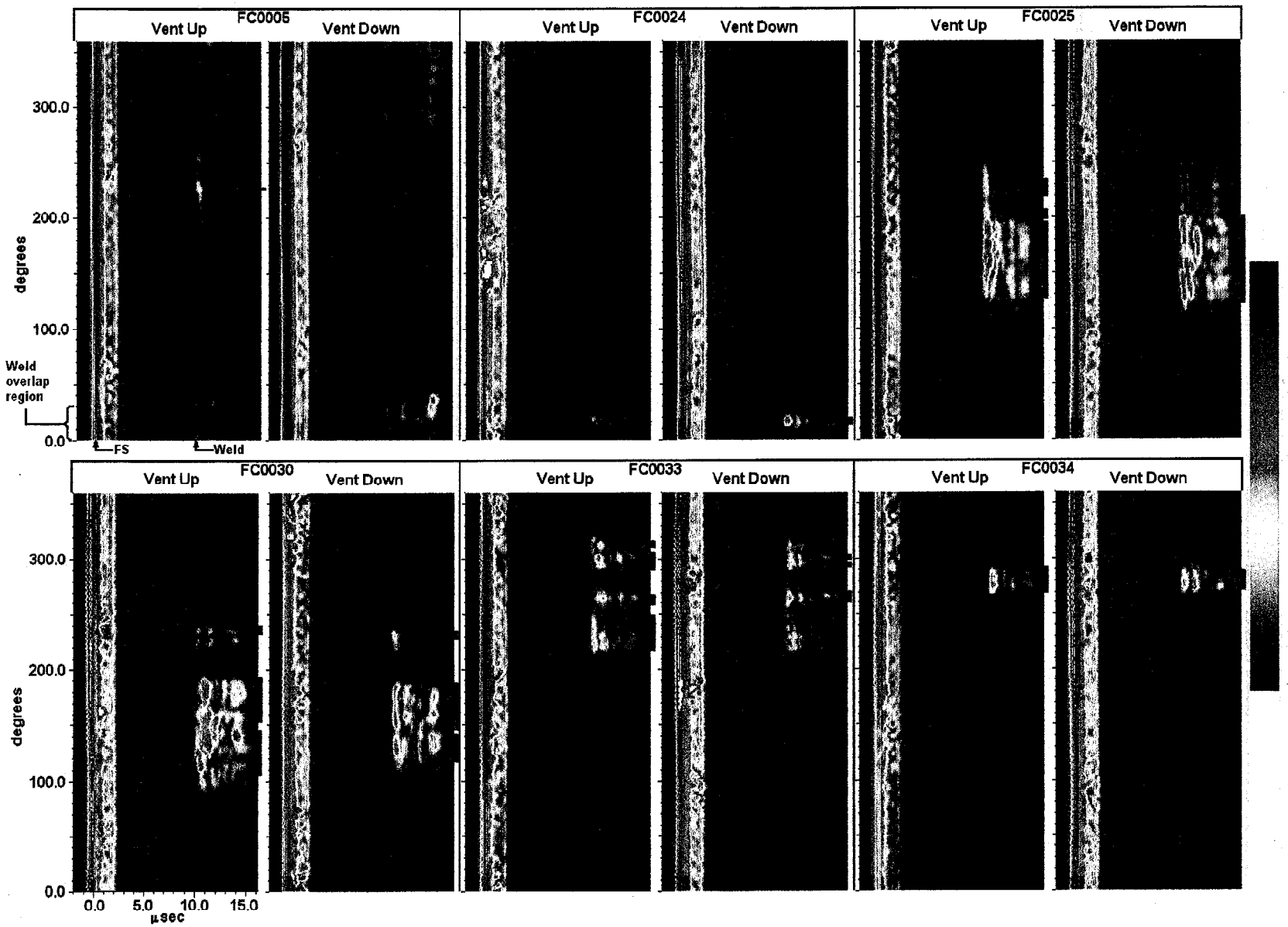

Figure 17-- B-Scan Plots from Fueled clads FC0005, FC0024, FC0025, FC0030, FC0033 and FC0034

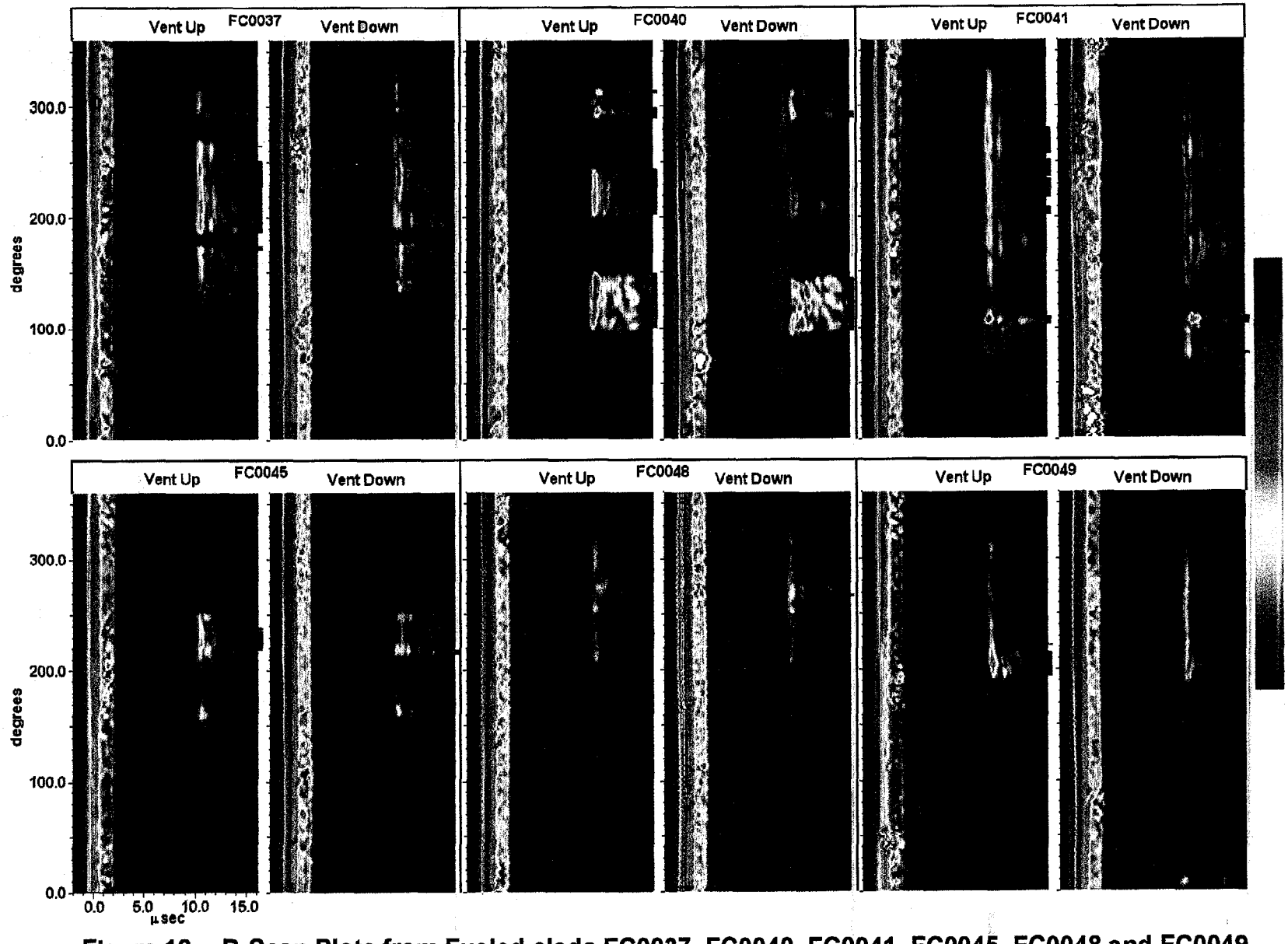

Figure 18 -- B-Scan Plots from Fueled clads FC0037, FC0040, FC0041, FC0045, FC0048 and FC0049

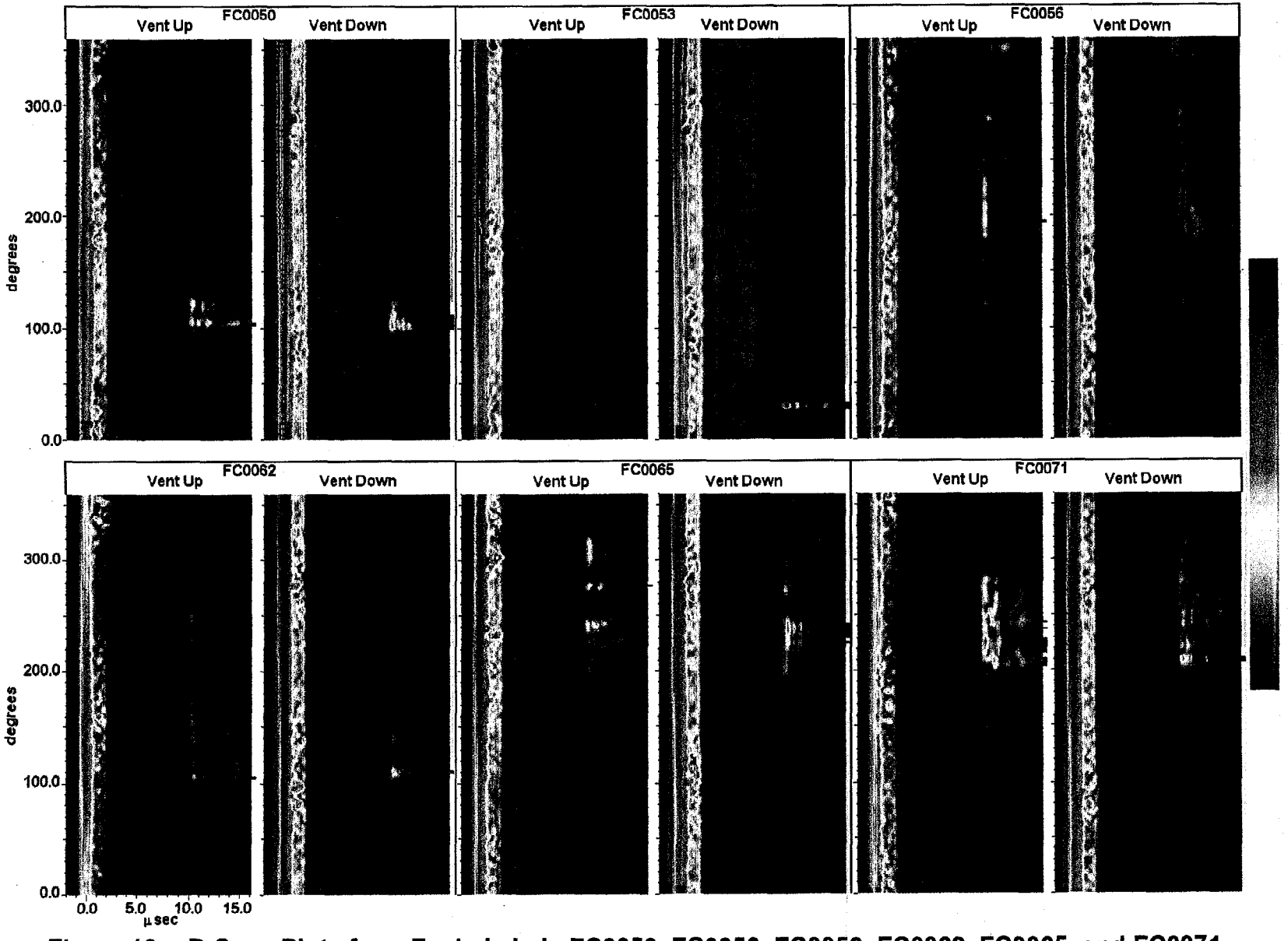

Figure 19 -- B-Scan Plots from Fueled clads FC0050, FC0053, FC0056, FC0062, FC0065, and FC0071

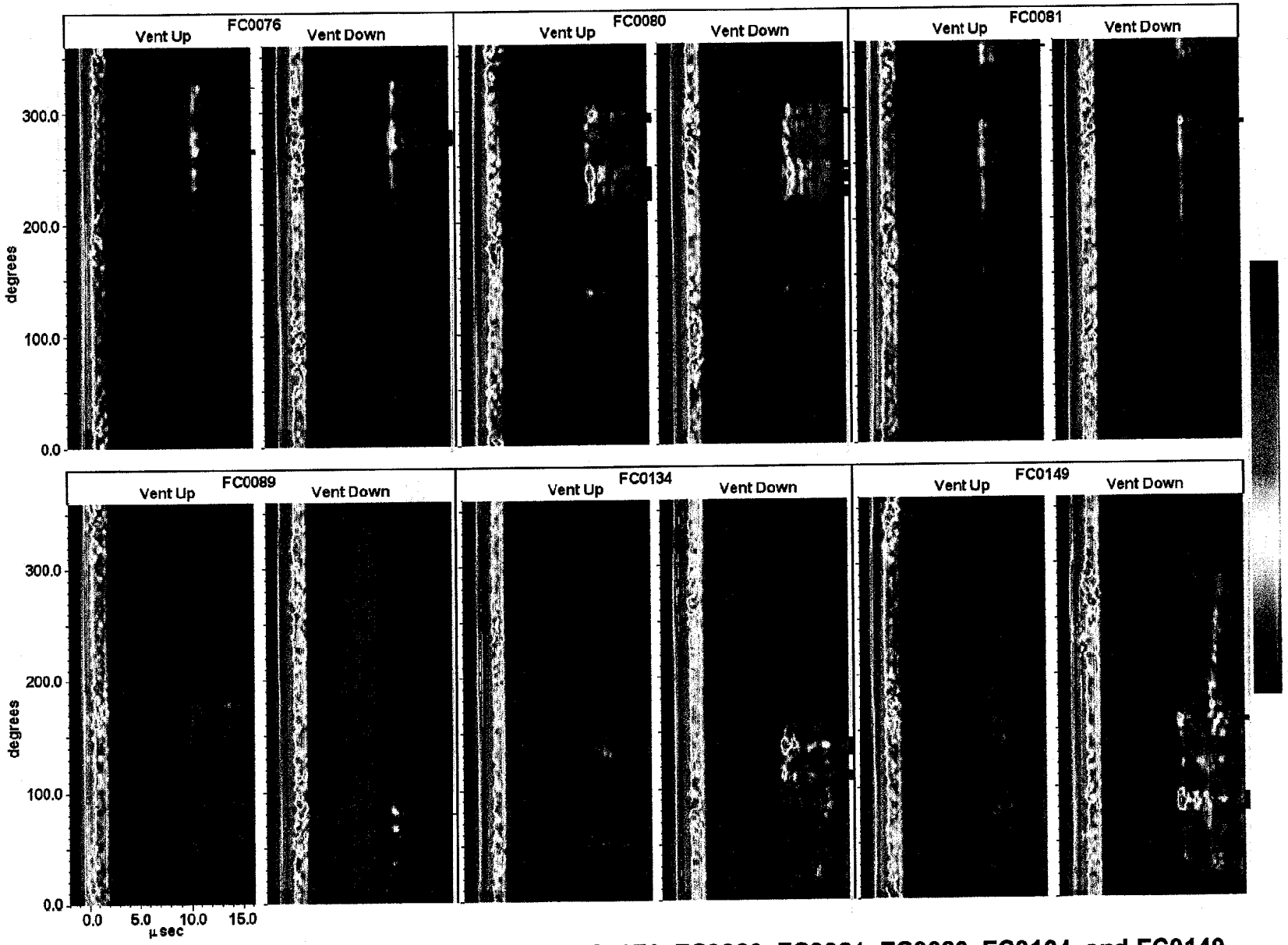

Figure 20-- B-Scan Plots from Fueled clads FC0076, FC0080, FC0081, FC0089, FC0134, and FC0149

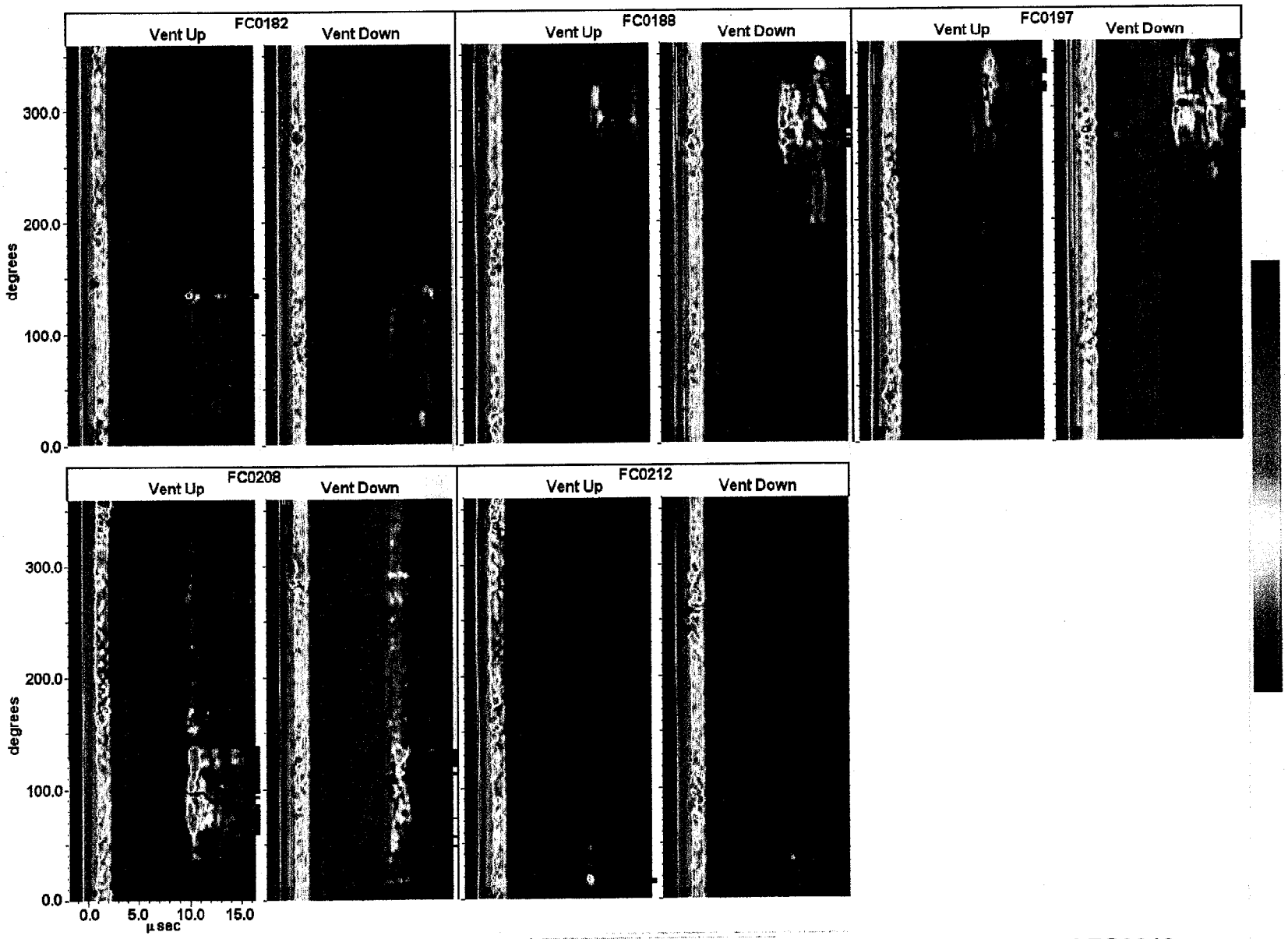

Figure 21 -- B-Scan Plots from Fueled clads FC0182, FC0188, FC0197, FC0208, and FC0212

The second class is long linear signals. Most of the fueled clads (all except FC0024, FC0034, FC0053, and FC0212) have this type of indication even though only short sections may be above the threshold.

We then break down these signals to further characterize them. First we look for easily identified curved signals occurring later in time (to the right in the B-scan plots). The signals may be in the Vent Up or the Vent Down scan or both. These are seen in fueled clads FC0025, FC0033, FC0037, FC0040, FC0041, FC0045, FC0048, FC0049, FC0056, FC0062, FC0065, FC0071, FC0080, and FC0081. These areas are identified as internal mismatch.

Next we look for well defined multiple reflections. These are found in fueled clads FC0025, FC0030, FC0034, FC0040, FC0041 FC0050, FC0071, FC0076, FC0149, FC0188, FC0197, and FC0208. Some fueled clads have both curved and linear areas. These areas are also identified as internal mismatch.

Next we look for areas that do not have well defined multiple reflections. In many cases, these signals will vary significantly in amplitude with small spots of high amplitude. I suspect that the weld shield is touching in the areas of low amplitude and actually fused to the spots of high amplitude. These conditions are found in fueled clads FC0005, FC0089, FC0134, FC0149, FC0182, and FC0208.

The identification of these areas of internal mismatch and weld shield fusion in the B-scan data is also summarized in Table 3.

Finally, we look at the larger signals and try to determine the weld condition in the area where these large signals occur. Most of the large signals are associated with well-defined geometric conditions. The short signals in the critical weld overlap region of fueled clads FC0024 and FC0053 have been described above. The area in fueled clad FC0034 is shorter than generally found but is away from the weld overlap region and has well defined multiple reflections. It was thus identified as internal mismatch. The short signals in fueled clads FC0041 and FC0049 are located at the end of a region of internal mismatch and are thus identified as belonging to a sharp geometric discontinuity associated with the mismatch.

Thus, we have been able to characterize most of the conditions found in the nonconforming fueled clads. With the exception of two fueled clads, all the indications appear to be caused by geometric conditions.

Tangential radiography is a useful tool to aid in the verification analysis of the ultrasonic results. Tangential radiography is not a replacement for ultrasonics because each radiograph looks at only two points 180° apart on the fueled clad and it would take too long to provide adequate coverage. In addition, tangential radiography cannot detect closed conditions such as cracks where there is no

void. The last four columns of Table 3 summarize the tangential radiography results.

Tangential radiography can detect variation in wall thickness. Those fueled clads identified in the IM column had internal wall mismatch. Tangential radiography can also identify if there is a gap between the weld shield and the capsule wall. If there is a gap, tangential radiography can also detect if the weld protrudes and touches the weld shield. The fueled clads where the weld shield touches the capsule wall or where the weld protrudes and touches the weld shield are identified in the ST column. The angle column shows the location of the tangential radiographs and the Comments column describes the results. One observation is obvious. Just because tangential radiography detects the shield touching or an internal mismatch doesn't necessarily mean that a large ultrasonic signal will be detected. If the step transition is smooth, the signal will be small. If the shield touches the wall there will be little ultrasonic reflection because there is a small air gap. If when the shield touches the weld we assume that there is weld shield fusion, then the reflection size will depend upon the gap between the capsule and the weld shield. There could also be the condition where the shield touches the weld but there is no weld shield fusion. Here the ultrasonic signal size would depend upon the amount of weld protrusion.

Comparing the ultrasonic and tangential radiography produces a reasonable correlation. For fueled clads FC 0030, FC0037 FC0040, FC0041, FC0049, FC0056 FC0076 and FC0080 tangential radiography confirmed the internal mismatch identified in the B-scans. For fueled clad FC0050 it appears that the short area identified in the B-scan as internal mismatch is cause by the overlap in the weld shield pressing against the weld. Thus this may be weld shield fusion instead of internal mismatch. For fueled clads FC0045 and FC0065, the tangential radiography identified points that were taken in areas that corresponded to B-scan signals as shield touching. The B-scan data identified these areas as internal mismatch. These areas had signals that were only slightly above the threshold and it is possible that there was a misidentification. However, in both cases the areas were identified as having benign geometric conditions. For the other fueled clads for which we have tangential radiographic data, the location of the radiographs is not identified.

Conclusions

The effort to inspect the GPHS fueled clads for the Cassini mission has been successful. We have developed an inspection that can easily inspect the closure weld and identify flight quality welds. We have found that there are a number of benign geometric conditions that can occur in welds that produce ultrasonic signals that are greater than the acceptance threshold. We have developed a B-scan inspection technique that can identify these conditions so that these fueled clads can be accepted for use.

This report has described the development of the ultrasonic inspection techniques, the analysis of the data and the evaluation protocol used to evaluate the B-scan data. We have confirmed the ultrasonic evaluation using tangential radiography in most cases.

For future missions it is possible that the inspection might be improved. With increased image processing capabilities it may be possible to automate the B-scan analysis protocol. It also may be possible to incorporate a normal inspection of the wall thickness adjacent to the weld to confirm the presence of internal mismatch.

ACKNOWLEDGEMENTS

The author wishes to thank the following personnel for their support for the development and implementation of the ultrasonic inspection of fueled clads for the Cassini Mission.

- W. J. Barnett and the Office of Space and Defense Power Systems for their support and vision for the Cassini Mission.
- T. G. George for his oversight of the program at Los Alamos.
- Arnost Placr for his interaction in the development of the ultrasonic inspection and for the suggestion of using the Top scan.
- Peyton Moore for his management of the Radioisotope Power Systems Program at ORNL and Y-12.
- W. A. Simpson for providing an analysis of Lamb wave propagation in the welded fueled clads and manuscript review.

The work described herein was conducted at

- Oak Ridge National Laboratory under DOE contract DE-AC05-96OR22464
- Y-12 National Security Complex under DOE contract DE-AC05-00OR22800

Internal Distribution

1. E. C. Fox
2. E. P. George
3. J. F. King
4-7. J. P. Moore
8-13. M. W. Moyer
14. E. K. Ohriner
15. M. L. Santella
16. G. B. Ulrich
17. Central Research Library
18. Laboratory Records – RC
19-20. Laboratory Records (OSTI)

External Distribution

21-27. U.S. Department of Energy, NE-50, Germantown Building, 11901 Germantown Road, Germantown, MD 20874-1290

C. E. Brown
L. W. Edgerly
L. C. Herrera
A. S. Mehner
W. D. Owens
R. C. Raczynski
E. J. Wahlquist

28. U.S. Department of Energy, Oak Ridge Operations Office, Bldg. 4500N, Mail Stop 6269, Oak Ridge, TN 37831

S. R. Martin, Jr.

29. U.S. Department of Energy, Miamisburg Office, P.O. Box 66, Miamisburg, OH 45342

T. A. Frazier

30-31. Babcock and Wilcox of Ohio, Inc., 1 Mound Road, Miamisburg, OH 45343-3000

D. M. Gabriel
J. R. McDougal

32. Lamb Associates, Inc., 1017 Glen Arbor Court, Dayton, Oh 4459-5421

E. W. Johnson

33. Lockheed Martin Astronautics, P.O. Box 8555, Philadelphia, Pa 19101

R. M. Reinstrom

34-36. Los Alamos National Laboratory, P.O. Box 1663, NMT-9, MS E502, Los Alamos, NM 87545

T. G. George
M. A. H. Reimus
E. M. Foltyn

37. Orbital Sciences Corporation, Inc., 20301 Century Blvd., Germantown, MD 20874

E. A. Skrabek

38. Teledyne Brown Engineering-Energy Systems, 10707 Gilroy Road, Hunt Valley, MD 21031

M. F. McKittrick

39. Westinghouse Savannah River Plant, Bldg 305-1A, Room 8, Aiken, SC 29808

Arnost N. Placr